Involvement of the Transmembrane Protein p23 in Biosynthetic Protein Transport

Manuel Rojo,* Rainer Pepperkok,‡ Gregory Emery,* Roland Kellner,§ Espen Stang,‖ Robert G. Parton,‖ and Jean Gruenberg*

*Department of Biochemistry, ‡Department of Cell Biology, University of Geneva, 1211 Geneva 4, Switzerland; §Institute of Physiological Chemistry and Patobiochemistry, Gutenberg Universität, 55099 Mainz, Germany; and ‖Centre for Microscopy and Microanalysis, Department of Physiology and Pharmacology, and Centre for Molecular and Cellular Biology, University of Queensland, Queensland 4072, Brisbane, Australia

Abstract. Here, we report the localization and characterization of BHKp23, a member of the p24 family of transmembrane proteins, in mammalian cells. We find that p23 is a major component of tubulovesicular membranes at the *cis* side of the Golgi complex (estimated density: 12,500 copies/μm^2 membrane surface area, or ≈30% of the total protein). Our data indicate that BHKp23-containing membranes are part of the *cis*-Golgi network/intermediate compartment . Using the G protein of vesicular stomatitis virus as a transmembrane cargo molecule, we find that p23 membranes are an obligatory station in forward biosynthetic membrane transport, but that p23 itself is absent from transport vesicles that carry the G protein to and beyond the Golgi complex. Our data show that p23 is not present to any significant extent in coat protein (COP) I-coated vesicles generated in vitro and does not colocalize with COP I buds and vesicles. Moreover, we find that p23 cytoplasmic domain is not involved in COP I membrane recruitment. Our data demonstrate that microinjected antibodies against the cytoplasmic tail of p23 inhibit G protein transport from the *cis*-Golgi network/intermediate compartment to the cell surface, suggesting that p23 function is required for the transport of transmembrane cargo molecules. These observations together with the fact that p23 is a highly abundant component in the intermediate compartment, lead us to propose that p23 contributes to membrane structure, and that this contribution is necessary for efficient segregation and transport.

TRANSPORT between different intracellular compartments is believed to be mediated by vesicular carriers that bud from one compartment and then specifically dock and fuse with the membrane of the target compartment (Palade, 1975). The combined efforts of genetics as well as in vivo and in vitro studies has led to the discovery of factors that actively participate in vesicle traffic. Most factors identified so far are proteins that cycle between a soluble, cytosolic form and a membrane-bound form while exerting their activity. Integral membrane proteins, however, are thought to confer ultimate membrane identity. They may function as membrane receptors for soluble factors, enable mutual recognition of membranes destined to fuse and perhaps catalyze the fusion process itself (Pryer et al., 1992; Pevnser and Scheller, 1994; Rothmann, 1994; Gruenberg and Maxfield, 1995).

Address all correspondence to J. Gruenberg, Department of Biochemistry, Sciences II, 30 quai Ernest Ansermet, 1211 Geneva 4, Switzerland. Tel. and Fax: 41-22-7042-64-64. E-mail: jean.gruenberg@biochem.unige.ch

R. Pepperkok's current address is ICRF 44, Lincoln's Inn Fields, London WC2A 3PX, Great Britain.

Recently, several new integral membrane proteins have been identified (Wada et al., 1991; Schimmöller et al., 1995; Stamnes et al., 1995; Belden and Barlowe, 1996; Blum et al., 1996; Fiedler et al., 1996; Sohn et al., 1996). They form a new family of proteins presumably implicated in vesicular traffic (Stamnes et al., 1995). This family is referred to as the p24 family; their members are small (≈24 kD), type I membrane proteins, with a short cytoplasmic tail (10–15 amino acids). They share at least 30% overall identity at the amino acid level, but the homology is significantly higher in certain domains (Stamnes et al., 1995; Sohn et al., 1996). Several members of this family contain conserved motifs in their cytoplasmic tails, including two lysine residues reminiscent of the di-lysine ER retention signal of type I membrane proteins (KKXX-CO_2) (Jackson et al., 1990).

Evidence obtained in yeast shows that members of the p24 family play a role in the secretory pathway. Indeed, yeast null mutants of the genes encoding for emp24p or erv25p, two members of the p24 family, display a selective delay in the secretion of a subset of proteins (Schimmöller et al., 1995; Belden and Barlowe, 1996). In addition, null

mutants of *EMP24* contain a reduced number of ER-derived transport vesicles (Stamnes et al., 1995) and are defective in the retention of ER resident proteins (Elrod-Erickson and Kaiser, 1996), suggesting that emp24p contributes to vesicle biogenesis and/or specific cargo selection. Moreover, since emp24p and erv25p are enriched in coat protein (COP)[1] II–coated vesicles generated in vitro (Schimmöller et al., 1995; Belden and Barlowe, 1996), these proteins have been proposed to function as receptors for coat proteins and/or cargo molecules on transport vesicles. Less is known about the mammalian p24 proteins. Peptides derived from the cytoplasmic tails of different p24 proteins have the capacity to recruit cytosolic COP I in vitro as efficiently as the KKXX-CO_2–motifs (Cosson and Letourneur, 1994; Fiedler et al., 1996; Sohn et al., 1996). One member of the family, p23, was shown to localize to the Golgi by immunofluorescence (Sohn et al., 1996), and to be enriched (together with p24) on COP I vesicles generated in vitro, suggesting that these proteins may function as COP I receptors (Stamnes et al., 1995; Sohn et al., 1996).

In this paper, we report the identification, localization, and characterization of BHKp23, the hamster ortholog of rabbit p23 (Sohn et al., 1996). We find that p23 is a, if not the, major component of *cis*-Golgi membranes that belong, in part, to the *cis*-Golgi network/intermediate compartment. We also find that p23 (*a*) is absent from vesicles that mediate transport between the *cis*-Golgi network/intermediate compartment and the Golgi complex; (*b*) is not required for membrane association of COP I; and (*c*) is not present in COP I–coated vesicles to any significant extent. Our microinjection studies indicate that p23 is involved in biosynthetic membrane transport. Altogether, our observations suggest that p23 plays a structural role in regulating the dynamics/organization of the *cis*-Golgi network/intermediate compartment membranes.

Materials and Methods

Cell Culture and Reagents

Monolayers of HeLa cells stably expressing a myc-tagged version of 1,2 *N*-acetylglucosaminyltransferase I (NAGT I), of BHK cells, and of CHO cells, were grown and maintained as described (Gruenberg et al., 1989; Nilsson et al., 1993). Vero cells were maintained and infected with tsO45 vesicular stomatitis virus (VSV; Indiana Serotype) as described (Kreis, 1986). For incubation of cells at 15°, 20°, or 31°C, cell culture medium was replaced by MEM containing 10 mM Hepes, pH 7.4, and 5 mM glucose. Cycloheximide, brefeldin A (BFA), and nocodazole were from Sigma Chemical Co. (St. Louis, MO); stock solutions (cycloheximide: 10 mg/ml in water; BFA: 5 mg/ml in methanol; and nocodazole: 10 mM in DMSO) were kept at −20°C.

Subcellular Fractionation, Electrophoresis, and Microsequencing

BHK cells were homogenized in isotonic sucrose solution and the membranes of the postnuclear supernatant were fractionated using a flotation step sucrose gradient (Aniento et al., 1993, 1996). In some experiments, membrane fractions were further sonicated for 5 min in 0.1 M carbonate, pH 11, and then centrifuged at high speed. Supernatants and pellet fractions were then analyzed in two-dimensional (2D) gel electrophoresis. Proteins that were both highly enriched in the pellet fraction and absent from the soluble fraction were considered as integral membrane protein candidates.

A combination of IEF and SDS-PAGE (Celis et al., 1990) was used to resolve proteins in high resolution 2D gels (Emans et al., 1993). The diameter of the IEF preparative gels (loaded with 1 mg protein) was 3.6 instead of 2.5 mm. Preparative SDS-PAGE gels were stained for 10 min in 45% methanol, 7.5% acetic acid, containing 0.25% Coomasie brilliant blue R-250. Gels were destained in 45% methanol, 7.5% acetic acid, washed extensively with water, and then dried under vacuum. Protein spots were cut out, rehydrated in SDS-PAGE sample buffer, and then incubated at 95°C for 15 min; the spots of up to 10 gels were concentrated with a second SDS-PAGE. To avoid protein dilution by band broadening, the stacking (3% acrylamide) and separating (8% acrylamide) gels were limited to the width of the sample with spacers. Concentration gels were run at constant voltage (40 V), and processed as before, but were not dried. The protein band was digested in matrix with trypsin. Fragments were separated by reverse phase HPLC and sequenced by Edman degradation (Emans et al., 1993).

COP Recruitment onto Membranes and Formation of COP-coated Vesicles In Vitro

The membrane recruitment of cytosolic COP I and the formation of COP I–coated vesicles was studied in vitro by incubating membranes (0.1 mg/ml) with rat liver cytosol (3.6 mg/ml) in the presence of an ATP-regenerating system and guanosine 5′-*O*-(3-thiotriphosphate) (GTPγS) (20 μM) as described (Serafini et al., 1991; Sönnichsen et al., 1996). When indicated, the ATP-regenerating system and/or GTPγS were omitted. To study COP I membrane association, 200 μl of the reaction mixture were centrifuged (Airfuge; 30 psi, 6 min). The pelleted membranes were resuspended in isotonic sucrose solution, and resedimented at the same speed to wash unbound COP I. To study COP I–coated vesicles formed in vitro, we used the protocol of Sönnichsen et al. (1996). A 1-ml sample of the reaction mixture was layered on top of a step gradient comprising 0.75 ml 30%, 3 ml 35%, 3 ml 40%, 3 ml 45%, 1 ml 50% (wt/wt) sucrose in 250 mM KCl, 2.5 mM $MgCl_2$, 20 mM Hepes-KOH, pH 7.2, and centrifuged to equilibrium (SW41; 40,000 rpm, 24 h). Fractions (1 ml) were collected from the top, diluted with 150 mM KCl, 2.5 mM $MgCl_2$, 20 mM Hepes-KOH, pH 7.2, to ≤8% sucrose, and membranes were sedimented by centrifugation (TLA 100.3; 100,000 rpm, 10 min). Sedimented membranes were solubilized in SDS sample buffer and analyzed by SDS-PAGE and Western blotting.

cDNA Cloning and Expression

The nonredundant GenBank/EMBL/DDBJ database at NCBI was searched with the BLAST program for sequences containing the two peptide sequences of BHKp23. Several expressed sequence tags (ESTs) containing both peptide sequences were identified. A human EST clone (these sequence date are available from GenBank/EMBL/DDBJ under accession number T10797) was made available to us by G. Bell (Howard Hughes Medical Institute Investigator, University of Chicago, Chicago, IL). Two 16-bp PCR primers were designed for generation of a 340-bp PCR product using the human EST clone as a template. The PCR product, coding for part of the open reading frame of human p23, was ^{32}P-labeled using random hexamer labeling (T7QuickPrime®; Pharmacia Biotechnology Inc., Piscataway, NJ). The labeled PCR product was used to screen (Church and Gilbert, 1984: 58°C) 2×10^6 plaques from a λZAPII (Gigapack gold II; Stratagene, La Jolla, CA) cDNA library from BHK cells. 20 out of 76 positive plaques were purified, converted to pBluescript KS (Stratagene), and analyzed by sequencing. All clones were identical in sequence; six were not truncated at the 5′-end and coded for a starting Met within a consensus Kozak (1989) sequence. One of the latter clones was sequenced in both directions using sequenase (Amersham Corp., Arlington Heights, IL) and custom oligonucleotide primers using a PRISM 310 Genetic Analyzer (Applied Biosystems, Inc., Foster City, CA).

Antibodies

Antibodies were raised in rabbits against two peptides within the luminal domain of BHKp23 (antibodies against luminal peptide 1 [LP1]: KNYEE-

1. *Abbreviations used in this paper*: BFA, brefeldin A; COP, coat protein; CT, antibodies against a peptide corresponding to the cytoplasmic tail of BHKp23; EST, expressed sequence tag; GTPγS, guanosine 5′-*O*-(3-thiotriphosphate); LP1 and LP2, antibodies against luminal peptides 1 and 2; NAGT I, 1,2 *N*-acetylglucosaminyltransferase I; PFA, paraformaldehyde; 2D, two dimensional; VSV, vesicular stomatitis virus.

IAKVE, and against luminal peptide 2 [LP2]: RLEDLSESIVNDFAY), and against a peptide corresponding to the cytoplasmic tail of BHKp23 (CT: TWQVFYLRRFFKAKKLIE). For affinity purification, the antigens were coupled to Affi Gel 10 (Bio-Rad Laboratories, Hercules, CA) as described by the manufacturer; antibodies were then bound to the coupled antigen in 10 mM Tris, pH 7.4, and eluted with 0.1 M glycine, pH 2.5. Antibodies were biotinylated with biotinyl-ε-aminocaproic acid *N*-hydroxysuccinimide ester (Gruenberg and Gorvel, 1993). Fab fragments of antibodies were prepared with papain immobilized on beads (Pierce Chemical Co., Rockford, IL) according to the instructions of the manufacturer. Rabbit antisera against the EAGE epitope of β-COP (Pepperkok et al., 1993), the mammalian KDEL receptor, ERD2 (Griffiths et al., 1994), and TGN38 (Luzio et al., 1990) were gifts of T.E. Kreis (University of Geneva, Geneva, Switzerland), H.D. Söling (University of Göttingen, Göttingen, Germany), and G. Banting (University of Bristol, Bristol, United Kingdom), respectively. Mouse mAb against β-COP (maD: Pepperkok et al., 1993; and M3A5: Allan and Kreis, 1986), ERGIC-53 (G1/93: Schweizer et al., 1988), and β′-COP (CM1A10: Orci et al., 1993; Lowe and Kreis, 1996) were provided by T.E. Kreis, H.P. Hauri (University of Basel, Basel, Switzerland), and J. Rothman (Sloan-Kettering Institute, New York), respectively. Mouse mAbs that recognize the myc epitope (9E10: Evan et al., 1985), a cytoplasmic epitope of VSV-G (P5D4: Kreis, 1986), and an exoplasmic epitope of VSV-G (17.2.21.4: Gruenberg and Howell, 1985; and VG: Pepperkok et al., 1993) have been described. Fluorescein-labeled, anti–mouse IgG, rhodamine-labeled, anti–rabbit IgG, and fluorescein-labeled streptavidin were from Jackson Immunoresearch Laboratories, Inc. (West Grove, PA). Unspecific control rabbit IgGs were from Sigma Chemical Co.

Immunofluorescence Microscopy and Microinjection

Cells were grown on glass coverslips and fixed with either methanol (−20°C, ⩾5 min) or paraformaldehyde (PFA; 20°C, ⩾20 min). PFA-fixed cells were permeabilized for 5 min with 0.1% (wt/vol) saponin in PBS. Antibodies were diluted in 10% goat serum, 0.1% saponin in PBS. For double labeling with mouse and rabbit antibodies, cells were incubated with the mixture of primary antibodies for 30 min, washed three times with PBS, and then incubated with a mixture of fluorescein-labeled, anti–mouse IgG and rhodamine-labeled, anti–rabbit IgG for 20 min. For double labeling with two rabbit antibodies, cells were first decorated with one antibody, followed by rhodamine-labeled, anti–rabbit IgG, and then with biotinylated CT, followed by FITC-streptavidin. Except for microinjection experiments, samples were analyzed with a confocal laser scanning microscope (LSM 410 invert; Carl Zeiss Inc., Thornwood, NY) equipped with an argon and a helium/neon laser for double fluorescence at 488 and 543 nm. Fluorescein and rhodamine signals were recorded sequentially (emission filters BP510-525 and LP590) using ×63 or ×100 Plan-APOCHROMAT oil immersion objectives. For overlay, fluorescein and rhodamine images were adjusted to similar output intensities and merged with Photoshop 3.0 (Adobe Systems Inc., San Jose, CA) into a composite RGB image using a Power Macintosh 7500/100 computer (Apple Computer Co., Cupertino, CA). Capillary microinjection of antibodies into cells was performed with an automated microinjection system (Zeiss AIS; Carl Zeiss Inc.) (Ansorge and Pepperkok, 1988) as described (Pepperkok et al., 1993). Microinjection experiments were analyzed with an inverted microscope (Axiovert 135TV; Carl Zeiss Inc.) equipped with a cooled CCD camera (CH250, 1317 × 1035 pixels; Photometrics Ltd., Tucson, AZ, USA), controlled by a Power Macintosh 8100/100 (Apple Computer Co.). Images were further processed with the software package IPLab spectrum V3.0 (Signal Analytics Corp., Vienna, VA). Ts-O45-G specific cell surface labeling was quantified as described (Pepperkok et al., 1993). Briefly, cells were fixed with 3% PFA and incubated for 15 min with antibody 17.2.21.4 (specific for a luminal epitope of the viral glycoprotein), followed by a rhodamine anti–mouse secondary antibody. Microinjected antibodies were detected by subsequently permeabilizing the cells with 0.1% Triton X-100, followed by incubation with fluorescein anti–rabbit antibodies (Sigma Chemical Co.). Final figures were arranged with PowerPoint 4.0 (Microsoft, Bellevue, WA) and printed on a Kodak Digital Science 8650 PS Color Printer (Eastman Kodak, Rochester, NY).

Electron Microscopy

To label the endosomal compartments with an electron-dense marker, BHK cells were incubated for 60 min at 37°C in the presence of 5 nm BSA-gold (Ludwig et al., 1991). The cells were then washed in ice-cold PBS, and processed for cryosections and immunogold labeling as described (Griffiths et al., 1984). Membrane fractions were sedimented by centrifugation (TLS-55; 55,000 rpm, 30 min), and then the pellet was fixed at room temperature with 8% PFA in 250 mM Hepes, pH 7.4, for 1 h. The solution was replaced with fresh fixative and samples were fixed for at least another 24 h. Fixed fractions were then processed for immunoelectron microscopy as described (Bomsel et al., 1990). Cryosections of BHK cells were immunolabeled for p23 and ERD2. Over 200 immunogold particles were counted, and the percentage of gold particles associated with the different structures was calculated. In intact cells, continuities between membranes were more difficult to judge than in fractions and so colocalization of p23 and ERD2 was based on proximity of <100 nm. For quantitation of p23 labeling of the M2 fraction, cells were double labeled for p23 and ERD2 (untreated fractions), or p23 and β-COP (GTPγS-treated fractions). In each case, >300 p23 gold particles were counted. Positive colocalization was judged by the presence of p23 and ERD2/β-COP labeling on the same membrane. The average linear density of p23-labeling on isolated membranes was 100 gold particles/μm. Assuming a section thickness of 80 nm and a labeling efficiency of 10% (values that are in the range of previous estimates) (Griffiths, 1993), an estimate of 12,500 p23 molecules/μm^2 membrane surface area was obtained.

Analytical Techniques

For standard SDS-PAGE (Laemmli, 1970), Protean gel II minigel system (Bio-Rad Laboratories, Hercules, CA) was used. For Western blotting, proteins were transferred onto nitrocellulose (0.4-μm pore size, Schleicher & Schuell, Inc., Keene, NH) using a semi dry transfer chamber (Bio-Rad Laboratories), and then stained with PROTOGOLD® (British Bio-Cell International, Cardiff, United Kingdom). Antibodies were detected by chemiluminescence with SuperSignal™ (Pierce Chemical Co., Rockford, IL), protein was determined with bicinchoninic acid (Pierce Chemical Co.).

Results

p23 Is a Member of the p24 Family of Proteins

We identified in a light membrane fraction of BHK cells a polypeptide of 23 kD (see below, Fig. 1 *C*), which was resistant to membrane extraction by carbonate treatment at pH 11, a behavior characteristic for transmembrane proteins. The protein was relatively abundant, as it could be visualized by protein stain in a total cellular extract (not shown). Microsequencing of p23 revealed that two tryptic fragments (Fig. 1 *A*, *LP1* and *LP2*) corresponded to the sequences of several human ESTs. These ESTs shared sequence homology to emp24p, a yeast protein involved in biosynthetic membrane transport (Schimmöller et al., 1995). Several homologues of emp24p have been identified, including in mammalian cells, and all these form a novel family of transmembrane proteins (Fig. 1 *B*). We used nucleic acid probes generated from one human EST clone to screen a BHK cDNA library, and obtained several cDNA clones that were identical in sequence. They always coded for both peptide sequences (Fig. 1 *A*), but differed in length towards the 5′ end. The clones containing a putative initiator methionine within a consensus Kozak sequence (Kozak, 1989) coded for an open reading frame of 219 amino acids (these sequence data are available from GenBank/EMBL/DDBJ under accession number AJ001513). The open reading frame of the isolated cDNA clones was found to be >97% identical at the amino acid level to Tmp21, a protein by then identified in human and rat (Blum et al., 1996: these sequence data are available from GenBank/EMBL/DDBJ under accession numbers X97442 and X97443) and to rabbit p23 (Sohn et al., 1996; GenBank/EMBL/DDBJ under accession number X98303).

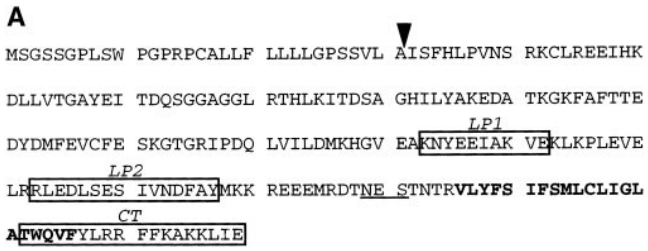

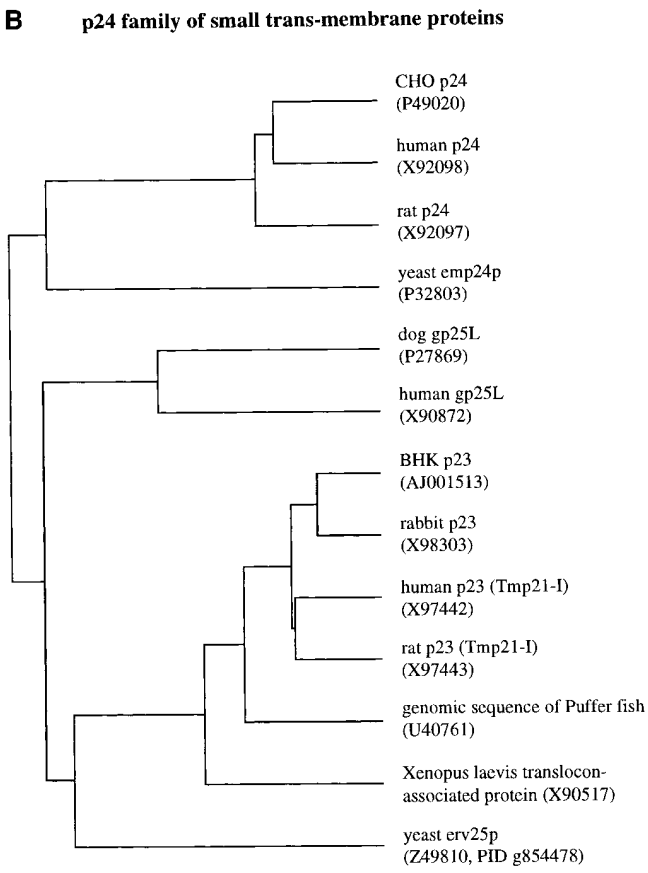

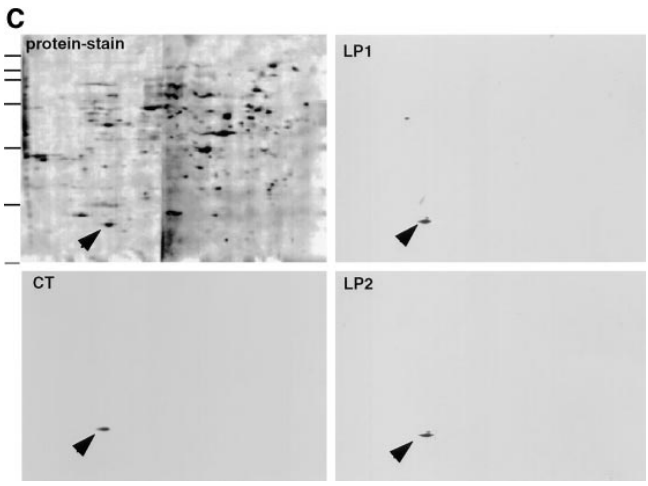

Figure 1. p23 is a member of the p24 family of proteins. (*A*) cDNA-derived amino acid sequence of the BHKp23 precursor. The predicted cleavage site for the signal peptidase is indicated by an arrowhead. The peptides used for generation of antibodies are boxed and their names given in italics. Peptides LP1 and LP2 were identified by microsequencing. The consensus site for glycosilation is underlined, the putative transmembrane domain is typed in bold characters. These sequence data are available from GenBank/EMBL/DDBJ under accession number AJ001513. (*B*) Dendogram of the p24 family. Only those proteins whose full-length sequence is known were analyzed, the accession numbers are indicated in parenthesis. Alignment and dendogram were performed with programs of Genetics Computer Group (Madison, WI). From the known yeast proteins mammalian p23 displays the highest similarity to yeast erv25p. (*C*) Characterization of antibodies against BHKp23. A membrane fraction enriched for p23 (interface M2 of Fig. 7) was subjected to 2D gel electrophoresis, blotted onto nitrocellulose, and then stained with PROTOGOLD (protein stain) or with LP1, LP2, or CT. The p23 protein (*arrowhead*) was already detected by protein stain and was specifically decorated with all three antibodies. Lines indicate the position of molecular mass markers (200, 116, 97, 66, 45, 31, and 22 kD).

BHKp23 exhibits significantly more homology to these three proteins (≥95%) than to any other member of the p24 family (20–30%; Sohn et al., 1996), indicating that it may correspond to the hamster ortholog of human/rat Tmp21 and rabbit p23 (Fig. 1 *B*).

The hydropathy analysis (not shown) revealed two strongly hydrophobic stretches: a putative transmembrane domain near the COOH terminus (Val186–Phe206/Leu208) and a predicted signal peptide at the NH_2 terminus (Met1-Ala31; Nielsen et al., 1997). The type I membrane topology was confirmed by treating intact membranes with trypsin or proteinase K. Western blot analysis using antibodies against two NH_2-terminal epitopes (see below) revealed a small decrease in the relative molecular mass of p23 after protease treatment. In contrast, both NH_2-terminal epitopes were digested by proteases in the presence of detergent (not shown). The predicted values for molecular mass and isoelectric point of the mature polypeptide (21.7 and 6.03 kD) agreed well with those determined by 2D gel electrophoresis (Fig. 1 *C*, 24.0 and 6.5 kD). Although the amino acid sequence contains a consensus site for Asn glycosylation (Asn179) (Fig. 1 *A*), BHKp23 was not glycosylated in vivo: treatment with *N*-glycosidase F did not affect protein mobility in SDS gels (not shown), consistent with the fact that that Asn179 is too close to the transmembrane domain for glycosylation to occur (Nilsson and von Heijne, 1993).

p23 Localizes to Tubulovesicular Membranes and Cisternae at the cis Side of the Golgi Apparatus

To characterize p23, we generated several rabbit antisera. As antigens, we used the two luminal peptides that were originally microsequenced (compare with Fig. 1 *A*), and a peptide of the COOH-terminal domain (compare with Fig. 1 *A*). The antibodies were affinity purified and characterized by Western blot analysis of 2D gels of the light membrane fraction; the antibodies decorated p23 in a highly specific manner (Fig. 1 *C*). Moreover, both Western blot and immunofluorescence signals (see below) were abolished after competition with the immunogenic peptide (not shown).

Immunofluorescence with anti-p23 antibodies revealed perinuclear structures with a Golgi-like aspect in different cell types (Fig. 2, BHK and HeLa; see Fig. 7, CHO and

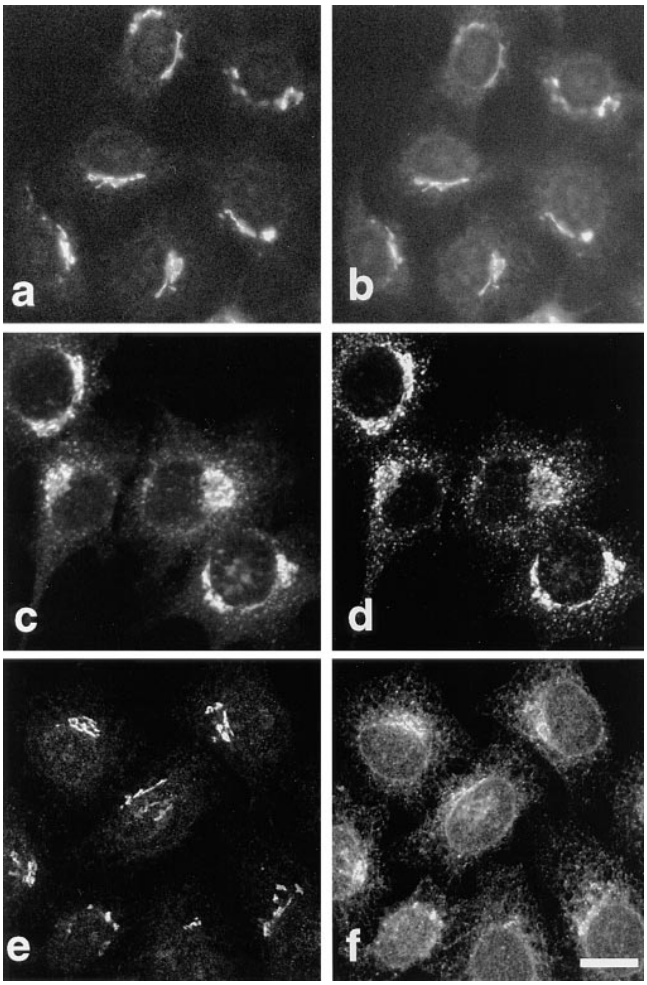

Figure 2. Immunolocalization of p23 to the perinuclear Golgi area. The p23 protein was decorated with antibody LP1 (*a* and *e*, HeLa) or CT (*c*, BHK). Double immunofluorescence with myc-tagged NAGT I (*b*), the KDEL receptor, ERD2 (*d*), and ERGIC-53 (*f*) is shown. Bar, 5 μm.

Vero; MDCK, not shown). Similar patterns were observed using two different antibodies, CT and LP1, and two different fixation protocols (PFA and methanol). This distribution closely resembled that of rabbit p23 (Sohn et al., 1996). As shown in Fig. 2, p23 overlapped with NAGT I (Fig. 2, *a* and *b*) and the KDEL-receptor ERD2 (Fig. 2, *c* and *d*). Whereas NAGT I is restricted to medial Golgi cisternae (Nilsson et al., 1993), the KDEL receptor, ERD2, has been localized both to the Golgi stack and to the intermediate compartment between ER and Golgi (Tang et al., 1993; Griffiths et al., 1994). In addition, p23 partially overlapped with ERGIC-53, but only within the perinuclear Golgi area (Fig. 2, *e* and *f*). Indeed, ERGIC-53 is used as a marker of the intermediate compartment (Schweizer et al., 1988, 1990), but the protein cycles between ER and Golgi (Lippincott-Schwartz et al., 1990) and a significant fraction of ERGIC-53 molecules localize to the ER at steady state in several cell types (Hans P. Hauri, personal communication) (Fig. 2 *f*, HeLa cells).

To better investigate the distribution of p23, we used nocodazole. This drug causes microtubule depolymerization and the appearance of small Golgi stacks scattered throughout the cytoplasm (Rogalski and Singer, 1984; Cole et al., 1996). After depolymerization of microtubules with nocodazole (not shown), p23 appeared scattered throughout the cytoplasm (Fig. 3), as did all Golgi markers we tested (Fig. 3). The p23 membranes were positive for both ERD2 (Fig. 3, *ERD2*) and ERGIC-53 (Fig. 3, *ERGIC-53*). Whereas the distributions of p23 and ERD2 largely overlapped (Fig. 3, *ERD2*), numerous ERGIC-53–positive membranes, presumably derived from the ER, were negative for p23 (Fig. 3, *ERGIC-53*). Within the dispersed Golgi stacks, p23 was partially segregated from the medial-Golgi enzyme NAGT I (Fig. 3, *NAGT I*) and completely separated from the *trans*-Golgi protein TGN38 (Fig. 3, TGN38) (Luzio et al., 1990). The differential degree of colocalization of p23 with proteins of the Golgi and of the *cis*-Golgi/intermediate compartment suggested that p23 localizes to the *cis* side of the Golgi apparatus.

The distribution of p23 was further investigated by immunogold labeling of BHK cryosections (Fig. 4). The label was exclusively found on tubulovesicular membranes at one side of the Golgi apparatus, as well as on cisternae of the Golgi stack (Fig. 4 *A*; Table I, *intact cells*). In good agreement with our immunofluorescence studies (Figs. 2 and 3), ERD2 colocalized with p23 on these membranes (Fig. 4 *B*). In fact, a quantitative analysis of the micrographs revealed that ERD2 and p23 colocalized to 100% (Table I, *intact cells*). Previous studies showed that the KDEL receptor, ERD2, localizes to the Golgi stack and to the intermediate compartment by immunoelectron microscopy (Griffiths et al., 1994), and to the *cis*-Golgi and the intermediate compartment by immunofluorescence (Tang et al., 1993). We can thus conclude that p23 localizes, together with ERD2, to tubulovesicular membranes and cisternae on the *cis* side of the Golgi, which may correspond to the ill-defined *cis*-Golgi network/intermediate compartment (Rambourg and Clermont, 1990; Schweizer et al., 1990).

After Brefeldin A or Low Temperature Treatments p23 Localizes to the Intermediate Compartment between ER and Golgi Apparatus

The distribution of p23 suggested that the protein localizes to early biosynthetic membranes at the *cis* side of the Golgi complex. BFA causes COP I release from Golgi membranes, and the relocalization of Golgi proteins to the ER (Klausner et al., 1992). In contrast, ERGIC-53/p58, ERD2, and other proteins of the *cis*-Golgi/intermediate compartment (gp74, p210, and GM130), remain well separated from the ER after BFA treatment (Lippincot-Schwartz et al., 1990; Saraste and Svensson, 1991; Tang et al., 1993; Alcalde et al., 1994; Rios et al., 1994; Nakamura et al., 1995). After treatment of HeLa cells with BFA, the distribution of COP I proteins changed within minutes from the typical Golgi pattern to a cytoplasmic staining (not shown), and NAGT I was relocalized to the ER (Fig. 5 *f*). In contrast, p23 did not redistribute to the ER, but appeared within discrete punctate structures (Fig. 5, *a*, *c*, and *e*), which were also positive for both ERGIC-53 (Fig. 5 *b*) and ERD2 (Fig. 5 *d*). These observations confirmed that ERGIC-53 (Lippincott-Schwartz et al., 1990; Saraste and

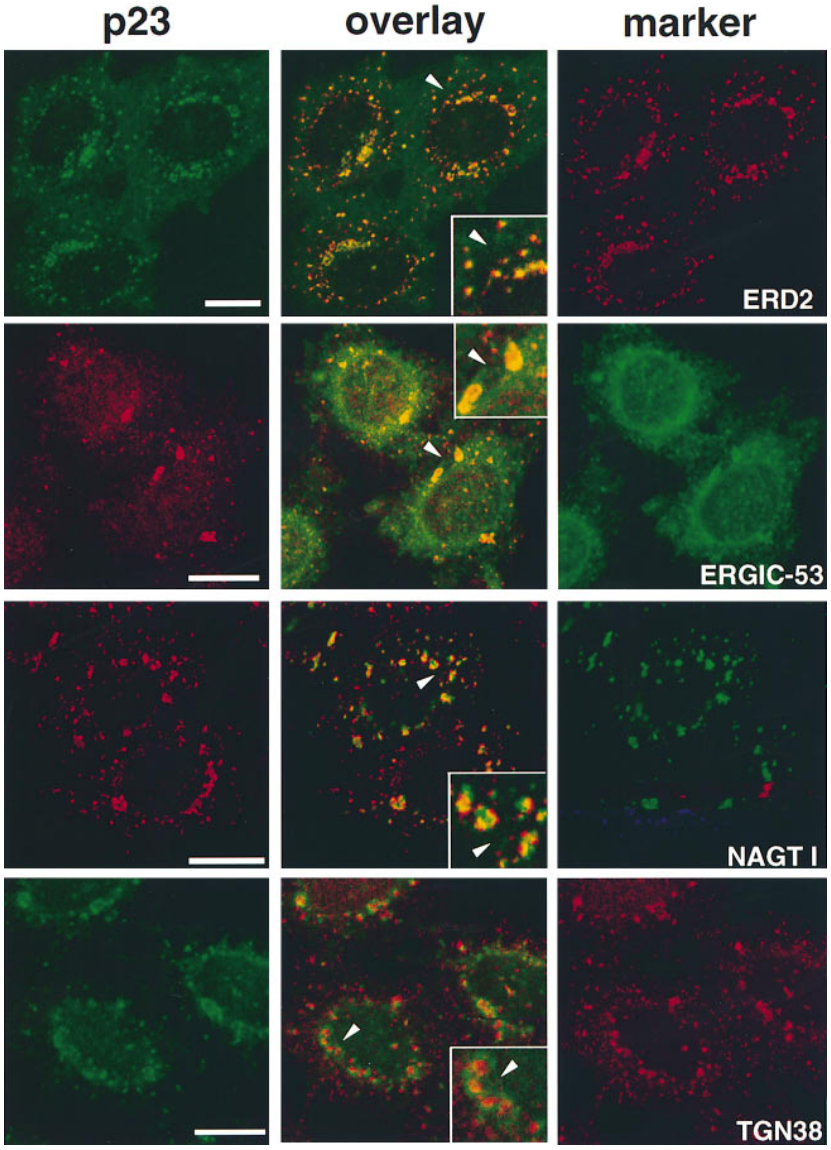

Figure 3. Immunolocalization of p23 after microtubule disruption with nocodazole. HeLa cells were treated with 10 μM nocodazole for 2 h to induce the formation of dispersed Golgi stacks, were fixed, and then processed for double immunofluorescence with antibodies against p23 and ERD2, ERGIC-53, myc-NAGT I, or TGN38. For double immunofluorescence of p23 with ERD2 or TGN38, biotinylated CT antibody was revealed with streptavidin-FITC. Fluorescein and rhodamine channels were merged (*overlay*) after adjustment of both fluorescence signals to similar levels. The inset shows a higher magnification of the area indicated by an arrowhead. The p23 signal overlapped completely with that of the KDEL receptor, ERD2, and extensively with that of ERGIC-53. Numerous ERGIC-53–positive membranes, corresponding to the ER, did not contain p23. Segregation of NAGT I and p23 occurred in perinuclear Golgi fragments that labeled for both markers, and in smaller peripheral structures that only labeled for p23. The absence of signal overlap between p23 and TGN38 was obvious. The colocalization of p23 with proteins of the *cis*-Golgi (*ERD2*), and the segregation of p23 and proteins of the medial (*NAGT I*) and *trans*-Golgi (*TGN38*) indicates that p23 localizes to the *cis* side of the Golgi. Bar, 5 μm.

Svensson, 1991) and ERD2 (Tang et al., 1993; Scheel et al., 1997) do not redistribute to the ER upon BFA treatment. Changes in p23 distribution caused by BFA may indicate that the steady-state distribution of p23 relies on constant (re)cycling between early biosynthetic compartments, as has been observed for other proteins with a similar subcellular distribution (compare with Lippincott-Schwartz et al., 1990; Alcalde et al., 1994). Alternatively, it is also possible that changes in p23 distribution caused by BFA are due to drug-induced changes in membrane organization. More importantly, these experiments showed that p23 exhibited the typical behavior of *cis*-Golgi/intermediate compartment proteins after BFA treatment.

The intermediate compartment was originally defined as the site where proteins destined to the plasma membrane accumulate at 15°C (Saraste and Kuismanen, 1984). We therefore investigated the relationships that may exist between p23 and the "15°C-intermediate compartment." We used the tsO45 mutant of the VSV glycoprotein G (tsO45-G), as a marker of the 15°C-intermediate compartment. The tsO45-G protein remains misfolded in the ER at the nonpermissive temperature of 39.5°C, and is properly folded and transported to the plasma membrane at 31°C (Bergmann et al., 1981). Like other cargo molecules, tsO45-G accumulates in the intermediate compartment at 15°C (Schweizer et al., 1990; Lotti et al., 1992; Pepperkok et al., 1993; Griffiths et al., 1995). Vero cells were infected with VSV tsO45, and then incubated at 39.5°C for 2.5 h to allow synthesis and accumulation of tsO45-G in the ER. Cycloheximide was added to inhibit further protein synthesis and the cultures were brought to 15°C for 3 h. Cells were then processed for immunofluorescence and decorated with antibodies against p23 an tsO45-G. As expected, tsO45-G accumulated in the intermediate compartment and did not reach the plasma membrane (Fig. 6, *0′*, *VSV-G*). More importantly, tsO45-G then colocalized with p23 in the intermediate compartment (Fig. 6, *0′*, *overlay*).

The effects of the "15°C block" are fully reversible and membrane traffic is re-established after shift back to 31°C (Saraste and Kuismanen, 1984). After release from the 15°C block, it is thus possible to analyze and compare the transport routes of different proteins (Griffiths et al., 1995;

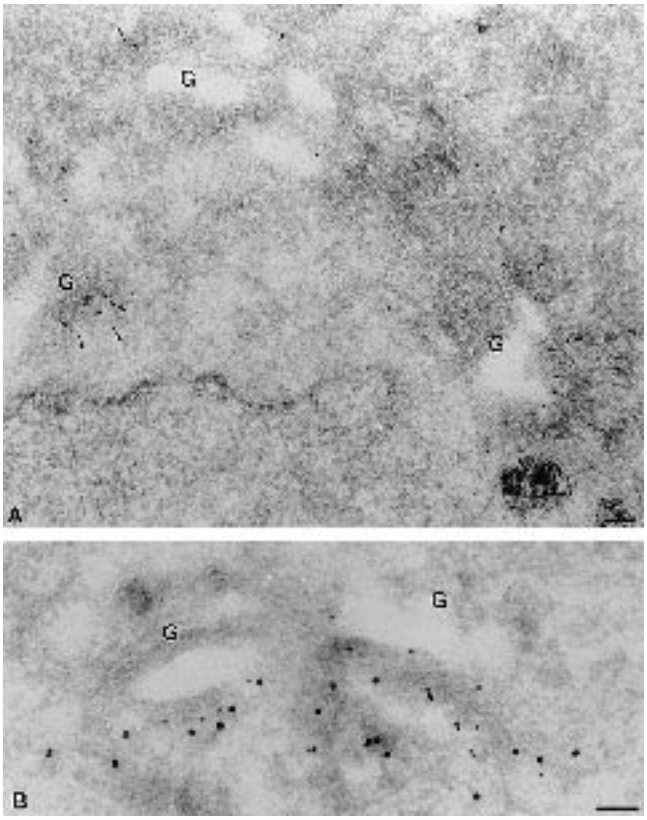

Figure 4. Localization of p23 to tubulovesicular membranes in the *cis* side of the Golgi. BHK cells were fixed and processed for frozen sectioning. *A* shows sections that were labeled with antibodies to p23 (CT) followed by 10 nm protein A–gold (*arrowheads*). Label is associated with tubulovesicular elements predominantly located in the vicinity of one face of the Golgi apparatus (*G*). Note the absence of labeling on other organelles including the ER surrounding the nucleus (*lower left*) and endosomes labeled with internalized 5 nm BSA-gold (*lower right*). *B* shows sections labeled with antibodies to p23 (CT; 15 nm gold) and to ERD2 (10 nm gold). The two antibodies colocalize on Golgi-associated membranes. Bar, 100 nm.

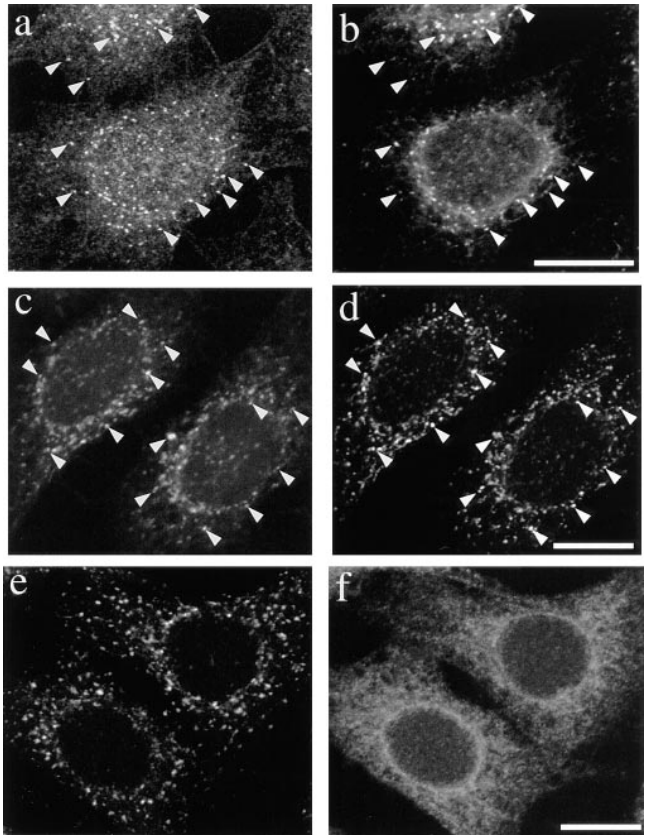

Figure 5. p23 localizes to the intermediate compartment after BFA treatment. HeLa cells were treated with 20 μg/ml BFA for 1 h and fixed with methanol (*a* and *b*) or PFA (*c–f*). Cells were double labeled with antibodies against p23 (*a*, LP1; *c* and *e*, CT) and ERGIC-53 (*b*), the KDEL receptor ERD2 (*d*) or myc-NAGT I (*f*). Whereas the medial Golgi enzyme NAGT I relocated to the ER (*f*), p23 appeared within discrete punctate structures scattered throughout the cytoplasm (*a*, *c*, and *e*), where it colocalized (*arrowheads*) with ERGIC-53 (*b*) and ERD2 (*d*). Bar, 5 μm.

Tang et al., 1995). After accumulation of tsO45-G at 15°C, cells were shifted to 31°C for different times, and then analyzed by immunofluorescence. Within 3 min after shift, numerous vesicles containing tsO45-G were observed, presumably corresponding to transport intermediates carrying tsO45-G towards the Golgi complex (Fig. 6, *3′*). Strikingly, these vesicles were devoid of p23 labeling, suggesting that p23 is absent from vesicles that carry tsO45-G beyond the intermediate compartment (see also Fig. 9). Between 12 and 30 min, the number of peripheral structures containing p23 but not ts045-G, probably corresponding to elements of the *cis*-Golgi and/or intermediate compartment, increased (Fig. 6, *12′* and *30′*). During the same time both labels tended to overlap in the crescent of perinuclear Golgi membranes. This overlap may not reflect p23 and tsO45-G colocalization, but the inability to discriminate

Table I. Quantitation of the Distribution of ERD2 and BHKp23

	In intact cells						In M2 fractions			
	Golgi region			ER	Other	Colocalization with ERD2	Cisternae and tubules	Vesicles	Other	Colocalization with ERD2
	Cist	*TubVes*	*Total*							
BHKp23	23	76	99	0	1	100	94	2	4	99
ERD2	19	79	98	1	1	—	91	2	7	—

Intact cells or M2 fractions were processed for cryosectioning and immunolabeled for ERD2 and BHKp23 as in the representative micrographs shown in Figs. 4 and 11. The distribution of ERD2 and BHKp23 was quantified as described in Materials and Methods. In intact cells the percentage of gold particles present on stacked cisternae (*Cist*) or tubulovesicular profiles (*TubVes*) in the Golgi region, endoplasmic reticulum (*ER*), and other membranes (*Other*) was quantified. In M2 fraction the percentage of gold particles present on cisternae and tubular profiles, vesicles (50–80 nm circular profiles), or other membranes was quantified.

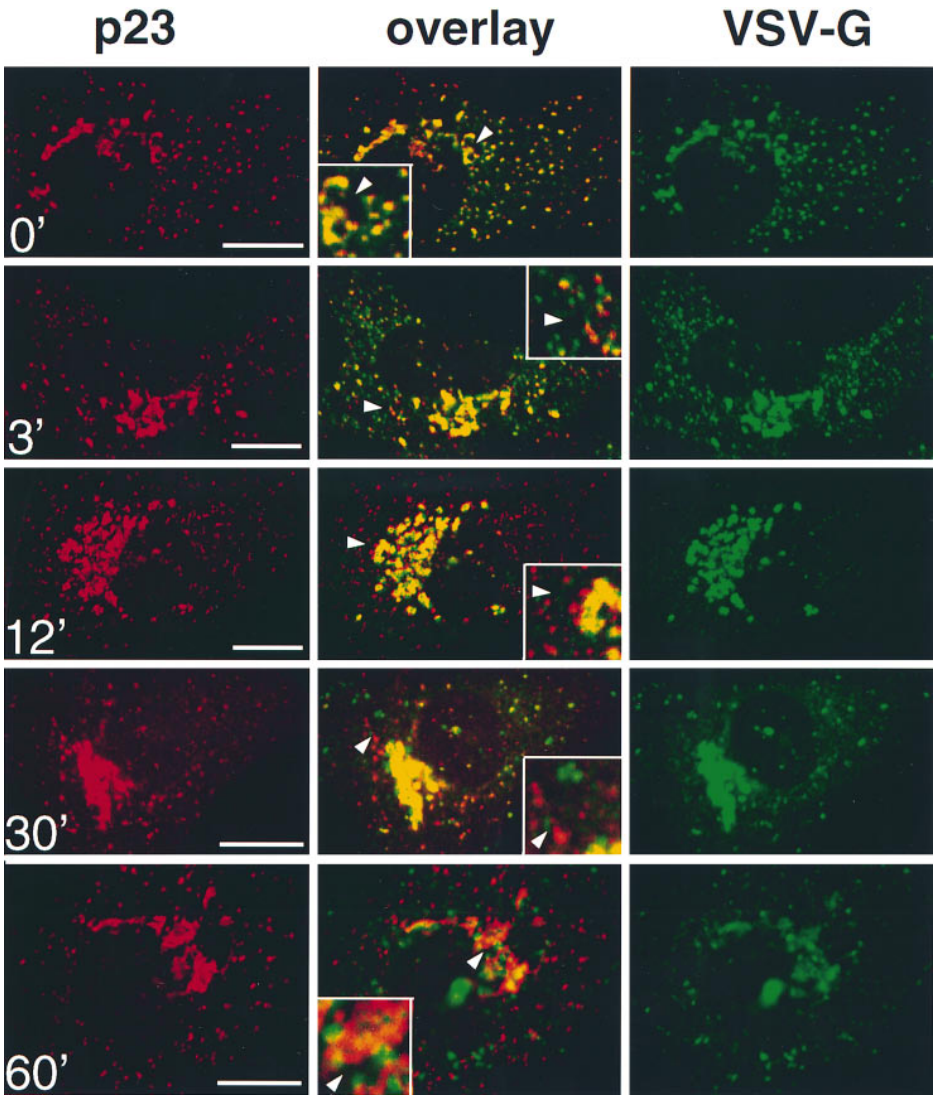

Figure 6. p23 colocalizes with VSV-G in the intermediate compartment at 15°C. Vero cells were infected with VSV tsO45 and maintained for 2.5 h at 39.5°C. Cycloheximide was then added, and tsO45-G was blocked in the intermediate compartment for 3 h at 15°C. The temperature was shifted to 31°C for the indicated periods of time, and cells were processed for double immunofluorescence with antibodies against p23 (CT) and VSV-G (P5D4). Images were processed and merged (*overlay*) as in Fig. 3. The inset shows a higher magnification of the area indicated by an arrowhead. VSV-G colocalized with p23 in the intermediate compartment at 15°C (*0′*). After release of the temperature block, forward transport of VSV-G resumed, and the degree of colocalization with p23 gradually decreased (*3′*, *12′*, *30′*, and *60′*). Bar, 5 μm.

between two close but separared fluorescent signals, as was observed for the steady-state distribution of *cis* and medial Golgi markers (Fig. 2). Beyond 30 min, little if any colocalization of the two proteins could be observed (Fig. 6, *60′*), while the bulk of tsO45-G had reached the plasma membrane (not visible in the confocal planes shown in Fig. 6). Altogether, these data indicate that p23 localizes to membranes that have been defined as intermediate compartment after BFA treatment or low (15°C) temperature incubations.

Subcellular Fractionation of p23

To better characterize the p23 protein and p23-containing membranes, we used subcellular fractionation. BHK cells were homogenized, a postnuclear supernatant was prepared and the membranes were separated by flotation in a step sucrose gradient (Aniento et al., 1993, 1996). Both p23 and ERD2 were highly enriched in the M2 interface (Fig. 7), in contrast to other proteins of the early biosynthetic pathway that are enriched in the M1 interface (ERGIC-53: Aniento et al., 1996; p97: Robinson et al., 1997). We also investigated the distribution of β-COP, a component of the COP I coat present on transport vesicles (for review see Kreis et al., 1995) that functions between Golgi stacks (Orci et al., 1989) and between ER and Golgi (Pepperkok et al., 1993; Letourneur et al., 1994). Whereas the bulk of β-COP was soluble after fractionation (Fig. 7), as expected, the membrane-associated form of β-COP was enriched in the M1 interface (Fig. 7), consistent with our previous findings (Aniento et al., 1996). These experiments show that both ERD2 and p23, which colocalized by immunofluorescence and immunogold labeling of cryosections, also codistributed by subcellular fractionation.

Localization of p23 and COP I

Electron microscopy studies have localized COP I to the Golgi complex and to the transitional area between ER and Golgi (Oprins et al., 1993; Griffiths et al., 1995). Moreover, Sohn et al. (1996) have reported that rabbit p23 is enriched in COP I–coated vesicles and that p23 cytoplasmic tail peptides have the ability to recruit COP I, leading to the proposal that p23 represents a Golgi-specific receptor for COP I that is involved in the formation of COP I–coated vesicles. We therefore compared the localization

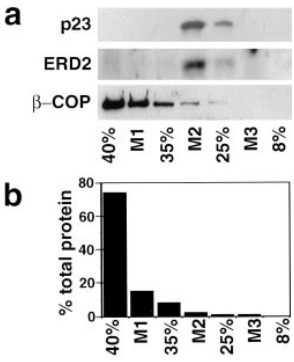

Figure 7. Cofractionation of p23 and ERD2. BHK cells were homogenized and membranes of the postnuclear supernatant were separated in a step sucrose gradient. In *a*, fractions were analyzed by Western blot (equal amounts of protein loaded per lane), and antibodies were revealed by chemiluminescence. In *b*, the protein content of each fraction is expressed as a percentage of the total amount in the gradient. The p23 protein and ERD2 were enriched in the M2 interface. Cytosolic proteins, including the bulk of β-COP (*a*), remained in the load of the gradient (*b*, *40%*).

of COP I with that of p23. Although both p23 and COP I exhibited a characteristic Golgi-like, perinuclear localization in different cell types, the distribution of the two proteins did not coincide (Fig. 8, *CHO*, *Vero*, and *HeLa*). This differential distribution was also evident after nocodazole-induced formation of dispersed Golgi stacks (Fig. 8, *HeLa [+nocodazole]*).

In the living cell, structures that appear to emanate from the 15°C-intermediate compartment upon release of this temperature block have been thoroughly characterized by fluorescence and electron microscopy (Griffiths et al., 1995). The majority of these structures is labeled for both cargo (tsO45-G) and COP I, suggesting that they represent tsO45-G–loaded, COP I–coated transport vesicles. We therefore investigated whether p23 was present on these COP I–labeled structures generated under identical conditions. Vero cells were infected with VSV tsO45, and

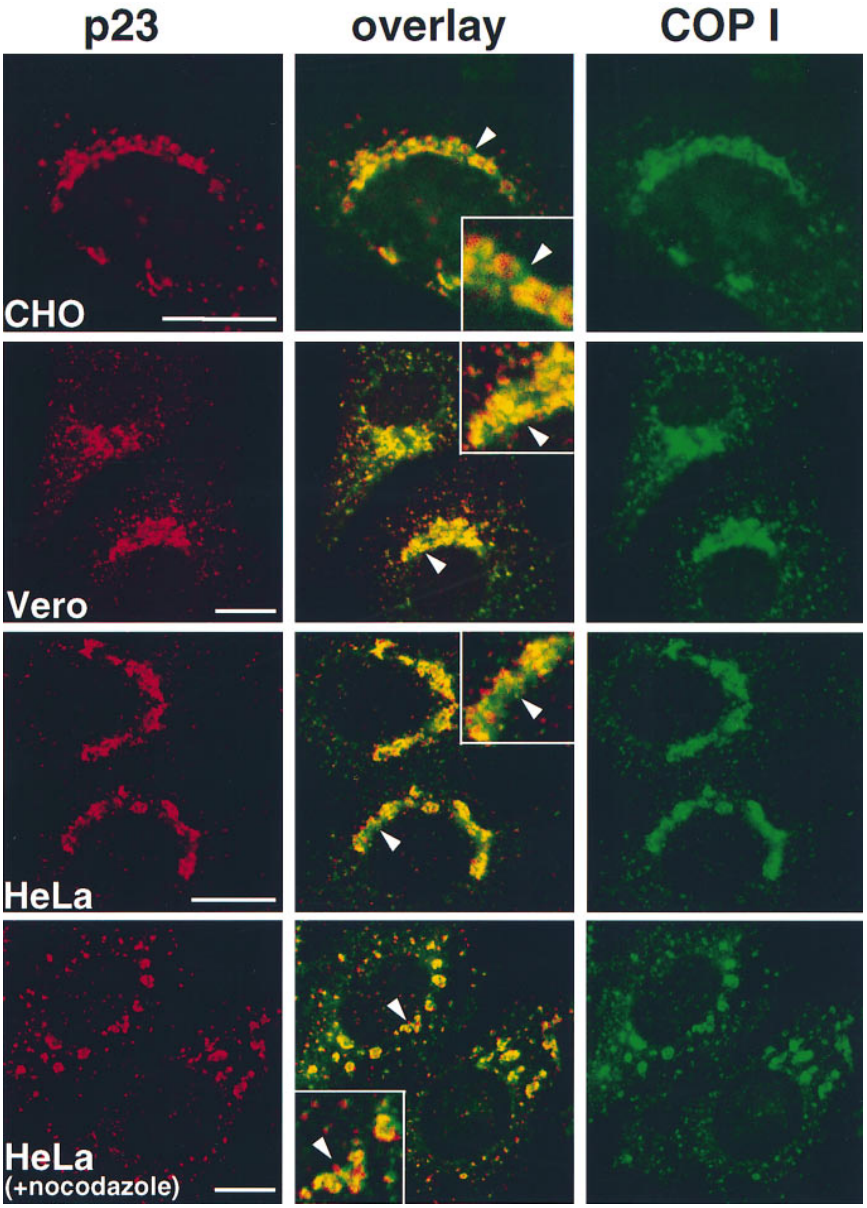

Figure 8. COP I and p23 distribution. The indicated cell types were fixed and processed for immunofluorescence, or treated with 10 μM nocodazole for 2 h before fixation (+ nocodazole). Images were processed and merged (*overlay*) as in Fig. 3. The inset shows a higher magnification of the area indicated by an arrowhead. Whereas both COP I and p23 localized to the perinuclear Golgi region in all cell types, the distribution of the two proteins was clearly different even in the absence of nocodazole. It is not clear to what extent overlapping signal (*yellow*) is due to colocalization of the proteins or to superimposition of two close but separated fluorescent signals. Bar, 5 μm.

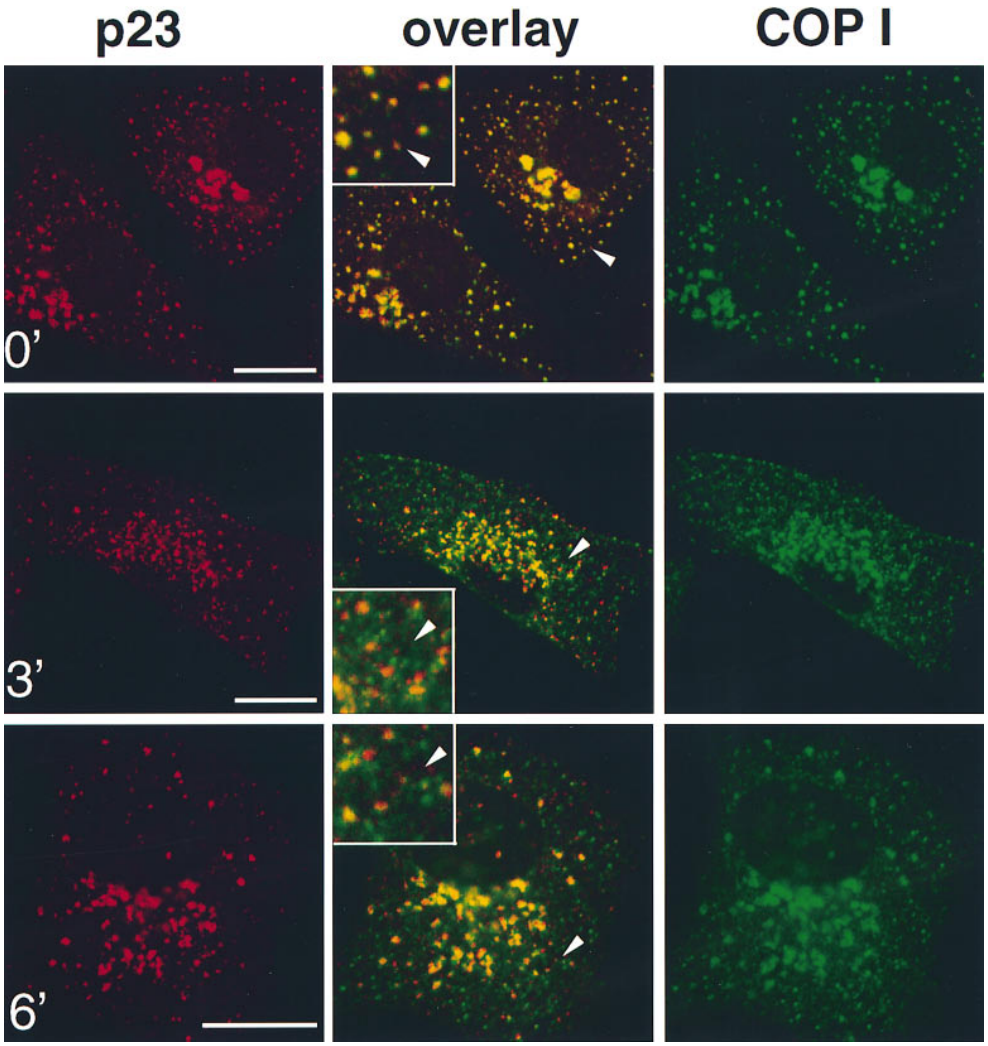

Figure 9. COP I and p23 colocalize in the intermediate compartment at 15°C, and segregate upon release of the temperature block. Vero cells were infected with VSV tsO45 and tsO45-G was blocked in the intermediate compartment for 3 h at 15°C as described in Fig. 6. The temperature was shifted to 31°C for the indicated periods of time, and cells were processed for double immunofluorescence with antibodies against p23 (CT) and COP I. Images were processed and merged (*overlay*) as in Fig. 3. The inset shows a higher magnification of the area indicated by an arrowhead. COP I and p23 colocalize in the intermediate compartment at 15°C (*0′*). Upon release of the temperature block (*3′* and *6′*), small COP I–positive structures, that may represent forward transport vesicles, are devoid of p23. Bar, 5 μm.

the tsO45-G protein was accumulated in the intermediate compartment at 15°C. Cells were then shifted to 31°C for different times and processed for immunofluorescence with antibodies against COP I and p23 (Fig. 9). We found that incubations at 15°C caused COP I to colocalize with p23 on intermediate compartment membranes (Fig. 9, *0′*), as predicted from the known effects of this temperature on COP I distribution (Griffiths et al., 1995). However, immediately after release of the temperature block numerous vesicles appeared that contained COP I, but were devoid of p23 (Fig. 9, *3′* and *6′*). These observations suggest that COP I–coated vesicles formed on the membranes of the intermediate compartment are devoid of p23, in agreement with our findings that vesicles carrying tsO45-G beyond the intermediate compartment do not contain significant amounts of p23 (Fig. 6, *3′*).

Interactions of COP I with p23 Membranes

Cytoplasmic tail peptides of p23 were reported to have the ability to recruit COP I in vitro (Sohn et al., 1996). We then investigated whether p23 interacted via its cytoplasmic domain with COP I proteins. In these experiments, we first tested the capacity of membrane fractions containing high amounts of p23 (M2) or essentially devoid of p23 (M1) to recruit cytosolic COP I in vitro. As shown in Fig. 10 *A*, the M1 and M2 fractions exhibited essentially the same COP I–binding capacity (Fig. 10 *A*, *β-COP*), despite the dramatic difference in their p23 content (Fig. 10 *A*, *p23*). To further investigate the role of p23, we repeated these experiments after BFA treatment of the cells in vivo. This treatment caused p23 to shift from the M2 to the M1 interface upon fractionation (Fig. 10 *A*, *p23*), presumably because BFA altered the physical properties of p23-containing membranes, by altering their protein composition through unbalanced transport. Enrichment of p23 was then lowered in M1 (when compared to M2 without BFA) because lanes were loaded with equal amounts of protein, and M1 contained more protein than M2 (Fig. 7 *B*). Despite the marked reduction of p23 content in M2 after the treatment, little, if any, difference could be observed in the COP I–binding capacity of the fraction. In the absence of GTPγS, significantly lower amounts of COP I were associated to membranes, suggesting that other factors, including ADP ribosylation factor (ARF) presumably, were rate limiting. Also this low, GTPγS-independent binding did not correlate with p23 distribution. It is conceivable that COP I binding properties, and perhaps the role of p23, are modified in the presence of excess ARF. In our experiments, however, cytosol was added in a 36:1 (mg protein)

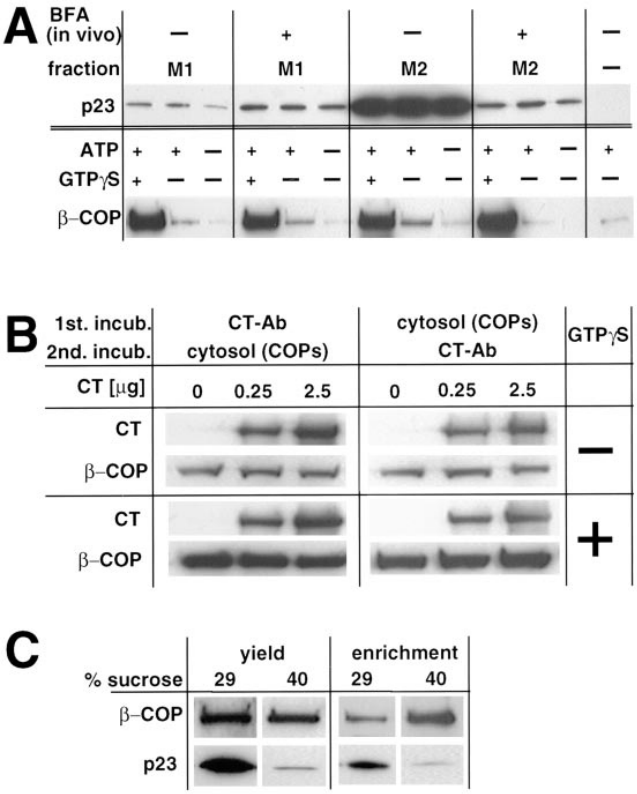

Figure 10. In vitro recruitment of COP I. (*A*) Membranes with low (*M1*) and high (*M2*) p23 content were prepared by subcellular fractionation. When indicated (+*BFA*), cells were pretreated with BFA to shift p23 from M2 to M1 membranes upon fractionation. To recruit COP I onto membranes, fractions (25 μg) were incubated with cytosol (900 μg) in the presence of the indicated nucleotides. Membranes were sedimented, washed, and analyzed by Western blot with antibodies against the indicated proteins. (*B*) Membranes (25 μg protein) with high p23 content (M2) were sequentially incubated; first with increasing amounts of CT, and then with cytosolic COP I or vice versa. Membranes were sedimented, washed, and analyzed as in *A*, using antibodies against rabbit IgG (to reveal bound CT) or against β-COP. To quantitate the binding of whole anti-p23 IgG molecules (CT), samples were not boiled in SDS. Lower exposures of this Western blot did not reveal any differences between untreated and CT antibody–treated membranes (not shown). (*C*) COP-coated vesicles were generated in vitro from donor M2 membranes in the presence of cytosol, ATP and GTPγS. The mixture was then centrifuged to equilibrium on a sucrose gradient as in Sönnichsen et al. (1996), and fractions were collected. Membranes of the donor fraction (*29% sucrose*) and of the COP vesicles fraction (*40%*) were sedimented and analyzed with antibodies against p23 and β-COP. Analysis of equal volumes of each fraction (*yield*) reveals that the bulk of p23 does not partition into COP I–coated vesicles. Analysis of equal protein amounts (8 μg; *enrichment*) shows that β-COP is enriched, and p23 is de-enriched, in COP–coated vesicles.

excess over membranes, and ARF is an abundant component of the cytosol. In any case, our experiments demonstrate that the COP-binding capacity of the membranes did not correlate with their p23 content. Furthermore, these experiments suggest that the cytoplasmic tail of p23 was not rate limiting for the association of COP I to membranes.

We then tested whether the CT antibody we raised against the cytoplasmic domain of p23 interfered with COP I binding onto membranes containing p23 (Fig. 7 *a*, *M2*). The CT antibody recognizes the cytoplasmic tail of p23 in Western blots (Fig. 1), in fixed cells (Figs. 2–9), in cells permeabilized with streptolysin O (unpublished), as well as in living cells after microinjection (see Fig. 12), and inhibits biosynthetic protein transport (see Fig. 12). Membranes (25 μg) were incubated with CT antibodies (0, 0.25, and 2.5 μg) for 2 h at 4°C, and then reincubated with cytosol as above and analyzed. Whereas the antibody clearly bound to membranes under all conditions (Fig. 10 *B*, *CT*), β-COP membrane recruitment in the presence or absence of GTPγS was completely unaffected by prebound CT antibody (Fig. 10 *B*, *β-COP*), even when using a large excess of CT (12.5 μg, not shown). Conversely, when the membranes were first incubated with cytosol to allow COP membrane binding to occur, and then with the CT antibody, no difference could be detected in antibody binding to the membranes (Fig. 10 *B*, *CT*). This was also true when COP prerecruitment had been stimulated with GTPγS (Fig. 10 *B*, *CT*). Control antibodies against a luminal peptide of p23, LP2, did not bind to membranes and were without effect on COP binding (not shown). We also found that preincubation of the cytosol with either 2 or 20 μM CT-peptide, or with control-peptide (LP2; compare with Fig. 1 *A*), had no effect on COP membrane binding (not shown). These experiments demonstrate that CT antibody and β-COP binding to membranes occur on different sites, and thus that the cytoplasmic tail of p23 is not required for the association of COP I proteins to membranes in vitro.

Finally, we investigated whether p23 was enriched in COP-coated vesicles generated in vitro, since enrichment of rabbit p23 in COP-coated vesicles formed in vitro has been reported (Sohn et al., 1996). We used the M2 membranes as donor membranes in the assay, since these contained the bulk of p23. Membranes were incubated with cytosol in the presence of GTPγS (Serafini et al., 1991; Sönnichsen et al., 1996), and then vesicles formed in vitro were purified by centrifugation on a sucrose gradient (Sönnichsen et al., 1996). After centrifugation, donor membranes and COP-coated vesicles were collected at 26–32% and 36–42% sucrose, respectively. Membranes were sedimented and analyzed by SDS-PAGE and Western blot. Donor membranes that had recruited β-COP clearly contained the bulk of p23 (Fig. 10 *C*, *yield*). In contrast, very little p23 could be detected in fractions containing COP I–coated vesicles formed in vitro (Fig. 10 *C*, *yield*). We then investigated whether p23, although present in low amounts, might be enriched in COP-coated vesicles, by comparing the p23 and COP content of equal protein amounts of donor membranes and coated vesicles (Fig. 10 *C*, *enrichment*). In contrast to β-COP, which was enriched in the vesicles formed in vitro, p23 was deenriched in COP-coated vesicles, when compared to donor membranes (Fig. 10 *C*, *enrichment*). Altogether these experiments demonstrate that BHKp23 is not involved in COP recruitment onto membranes and does not partition to any significant extent into COP-coated vesicles generated in vitro.

Ultrastructural Organization of p23 Membranes

As a next step, we analyzed the membranes highly en-

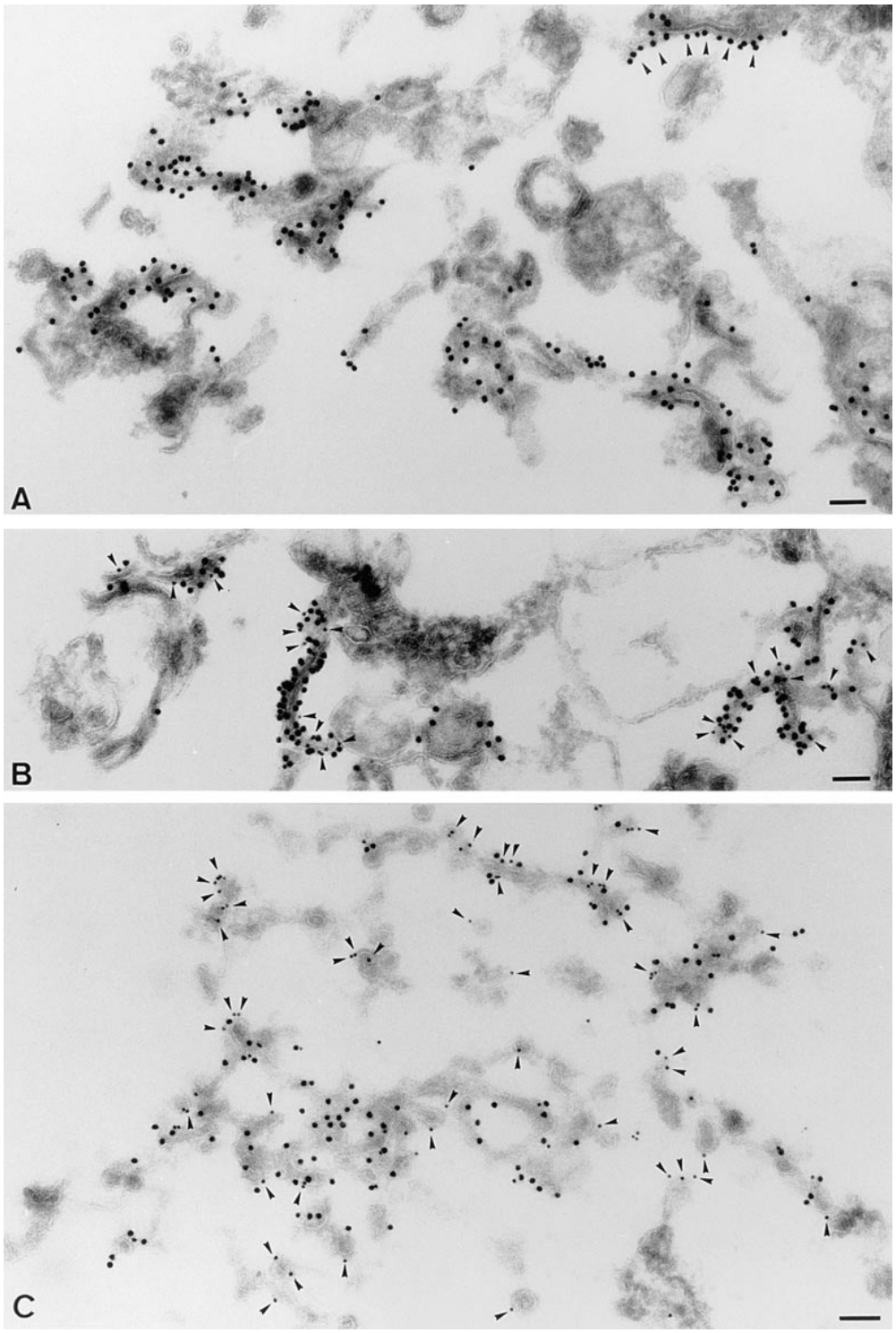

Figure 11. p23 is an abundant component of tubulovesicular or cisternal membranes that also contain the KDEL receptor, ERD2. Fractions enriched for p23 (fraction M2) were fixed and processed for frozen sectioning (*A* and *B*) or were treated with GTPγS in the presence of cytosol before fixation (*C*). *A* shows sections labeled for p23 (CT; 15 nm protein A–gold). Dense labeling is associated with the cytoplasmic surface of abundant tubular profiles (indicative of either cisternal elements or tubules). Note that the labeling sometimes appears to show polarized distribution lining only one surface domain of the tubule (e.g., *arrowheads*). *B* shows a section labeled for p23 (CT; 15 nm gold) and ERD2 (10 nm gold; *arrowheads*). The two markers colocalize on tubular elements. *C* shows a fraction incubated with GTPγS and cytosol before fixation. The section was labeled with antibodies to p23 (CT; 15 nm gold) and β-COP (EAGE-epitope, 10 nm gold; *arrowheads*). The two proteins show colocalization on tubular elements, but COP-labeled buds and vesicles are negative for p23. Bar, 100 nm.

riched in both ERD2 and p23 (Fig. 7 *b*, *M2*) by immunogold labeling of cryosections. Strikingly, p23 labeling was restricted to a discrete subset of membranes whose structure was reminiscent of cisternae or tubules (Fig. 11 *A*; Table I, *M2 fractions*), and very few gold particles were found on vesicular membranes (Table I, *M2 fractions*). As shown in Fig. 11 *B* (*arrowheads*), all p23-positive membranes also contained ERD2 (see Table I for quantification). Thus, this electron microscopy analysis of the fractions not only confirmed our observations that ERD2 and p23 colocalize in the same intracellular compartment (Figs. 2–5), but demonstrated that they distribute to the very same membranes.

Immunogold labeling of the isolated membranes was significantly improved, when compared to intact cells (compare with Fig. 4), presumably because of better antigen accessibility after cell homogenization (Griffiths, 1993). This analysis thus also revealed that p23 was extremely

Table II. Quantitation of the Distribution of COP I on Structures Labeled with p23 After GTPγS Treatment

	Cisternae		Vesicles/buds	
	p23+	p23−	p23+	p23−
COP I	14	0	7	79

M2 fractions were incubated with GTPγS, processed for cryosectioning, and then immunolabeled for p23 and β-COP (as in the representative micrograph shown in Fig. 11 *C*). The distribution of β-COP and BHKp23 to cisternal elements or vesicles and buds was quantified as described in Materials and Methods. The percentage of β-COP gold particles (*COP I*) associated with p23-positive (*p23+*) or negative (*p23−*) profiles was calculated.

abundant on these *cis*-Golgi network/intermediate compartment membranes. We could estimate that the density of p23 corresponded to 12,500 molecules/μm^2 membrane surface area (Materials and Methods), and thus that p23 may account for up to 30% of the total integral membrane proteins in these membranes (Quinn et al., 1984).

We have established that p23 membranes were able to recruit COP I coats (Fig. 10), but that the cytoplasmic domain of p23 was not involved in this process (Fig. 10, *A* and *B*). We also established that p23 molecules did not preferentially partition into COP I–coated vesicles (Fig. 10 *C*). When analyzed by electron microscopy, p23 membranes were devoid of β-COP (not shown), in agreement with our fractionation studies (Fig. 7). To further characterize the recruitment of COP I coats, p23 membranes of the M2 fraction (Fig. 7) were incubated with cytosol, an ATP-regenerating system, and GTPγS as described above. Membranes were sedimented, and analyzed by electron microscopy using antibodies against β-COP and p23. As expected, in addition to tubulovesicular membranes, numerous coated buds and vesicles were then visible (Fig. 11 *C*). Fig. 11 *C* clearly shows that p23 and β-COP (*arrowheads*) colocalized on tubular elements, demonstrating that p23 membranes were competent to recruit COP I, as shown in Fig. 10. In contrast, a quantitative analysis demonstrated that the vast majority (≈80%) of COP I–positive vesicles and buds were negative for p23 (Fig. 11 *C*; and Table II). These observations strongly suggest that the fraction of p23 incorporated within COP I–coated membranes was too low to be detected. In good agreement with our biochemical studies (Fig. 10 *C*), this morphological analysis confirmed that p23 was less abundant on COP I–coated vesicles than on purified p23 membranes.

Antibodies Against the Cytoplasmic Tail of p23 Inhibit Transport of ts045-G through the cis-Golgi Network/Intermediate Compartment

Since we found that ts045-G transiently colocalized with p23 in the intermediate compartment between ER and Golgi apparatus (Fig. 6), we investigated whether p23 participated in ts045-G transport. Previous studies had shown that microinjection of specific antibodies is a powerful approach to study protein function in vivo. Indeed, microinjected antibodies against the cytoplasmic tail of VSV-G (Kreis, 1986) and against β-COP (Pepperkok et al., 1993) inhibit VSV-G transport to the cell surface. We therefore investigated whether microinjection of antibodies against the cytoplasmic tail of p23 affected transport of VSV-G to the plasma membrane.

In these experiments, tsO45-G was accumulated in the ER at 39.5°C, cells were microinjected with antibodies against the cytoplasmic tail of p23, cycloheximide was added, and then transport was allowed to resume by lowering the temperature to 31°C. Fig. 12 shows two identical microinjection experiments (*a* and *b*, and *c* and *d*). The micrographs reveal that microinjected antibodies bound to intermediate compartment membranes (Fig. 12, *a* and *c*, *arrowheads*), and that excess antibody remained soluble in the cytoplasm (Fig. 12, *a* and *c*). In microinjected cells, the amounts of tsO45-G that reached the plasma membrane 60 min after releasing the 39.5°C block were significantly lowered when compared to neighboring, non-microinjected cells (Fig. 12, *b* and *d*). More importantly, tsO45-G molecules that did not reach the plasma membrane accumulated in intracellular membranes where they partially colocalized with p23 (Fig. 12, *b* and *d*). Microinjection of control antibodies was without effects (not shown). Quantification of the rate of tsO45-G appearance on the cell surface confirmed that anti-p23 tail antibodies, but not control antibodies, significantly inhibited tsO45-G transport. After 60 min, ≈40% of VSV-G molecules had reached the cell surface, when compared to the control (Fig. 12 *e*). In contrast, microinjection of monovalent Fab fragments of the same antibodies did not affect tsO45-G transport to the plasma membrane to any significant extent (Fig. 12 *e*). It is possible that Fab fragments exhibited a decreased avidity/affinity for their antigen and were thus not as inhibitory as whole IgG molecules. However, microinjected Fab fragments also recognized their antigen on the membranes (not shown). The absence of an effect upon microinjection of Fab fragments thus suggests that the inhibition caused by the intact antibody does not solely rely on steric hindrance, for example by preventing binding of soluble factors to p23 cytoplasmic tail, but may be due to the cross-linking of p23 molecules in the plane of the membrane (Kreis and Lodish, 1986). These observations agree with our findings in vitro, showing that antibodies against the cytoplasmic tail of p23 bind to isolated p23 membranes, but do not interfere with COP I recruitment.

To more precisely characterize the site of p23 action in forward membrane transport, we then used the same strategy to study and compare the effects of anti-p23 tail antibodies on tsO45-G transport from the intermediate compartment to the plasma membrane. After accumulation in the ER at 39.5°C, cycloheximide was added, and ts045-G molecules were allowed to reach the intermediate compartment during a 3-h incubation at 15°C. Antibodies were then microinjected, and cells were further incubated at 31°C to allow membrane transport to resume. As shown in Fig. 12 *f*, microinjected antibodies, which decorated the intermediate compartment (not shown), inhibited forward transport of ts045-G molecules, whereas control antibodies were without effects. However, when cells were incubated for 3 h at 20°C, rather than 15°C, to allow transport of tsO45-G to the TGN before microinjection (Griffiths and Simons, 1986), antibodies were without effects on ts045-G appearance on the cell surface (Fig. 10 *g*). These experiments rule out possible nonspecific effects of the anti-BHKp23 tail antibodies, and indicate that p23 is involved in the transport of transmembrane cargo molecules from the intermediate compartment to the cell surface.

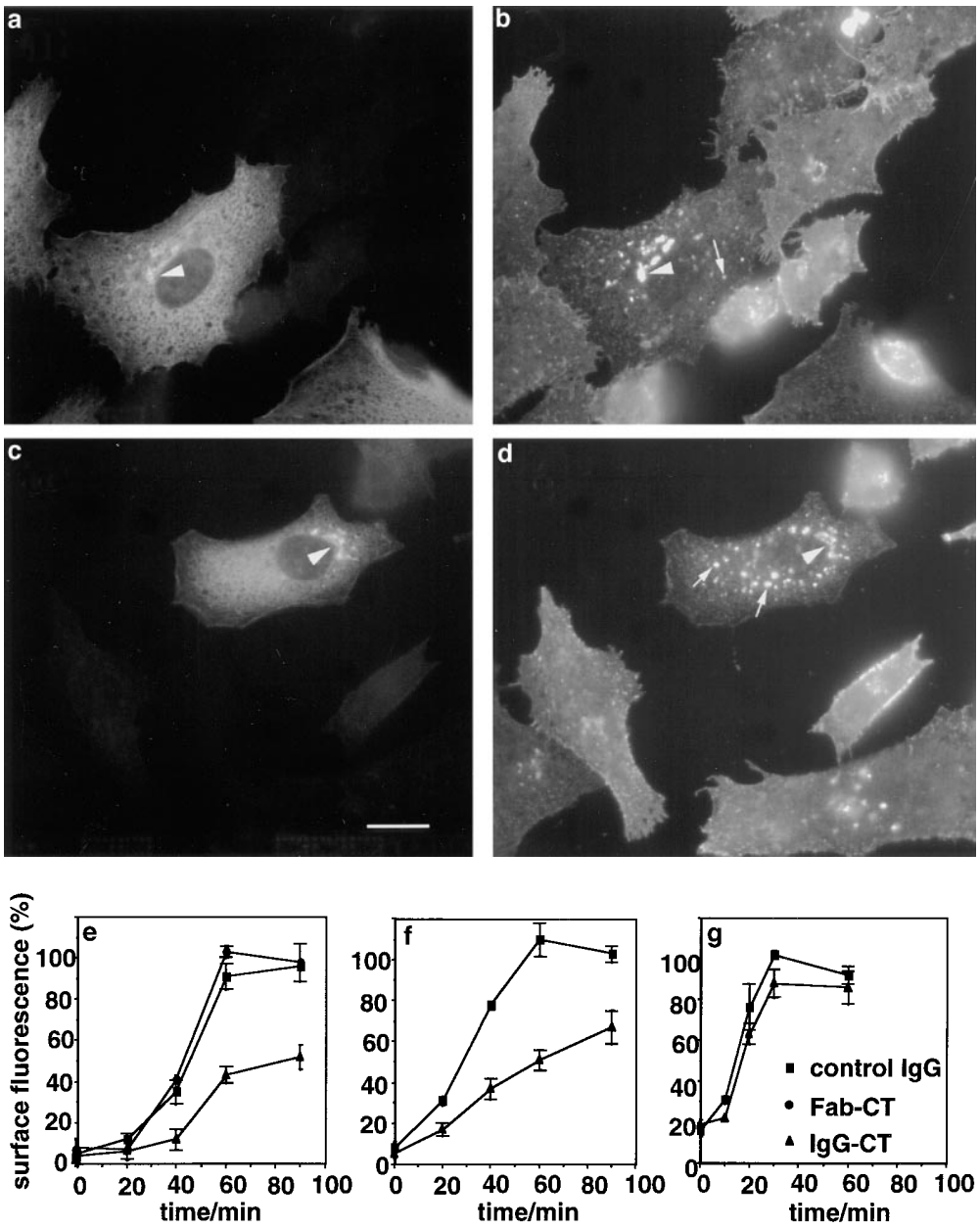

Figure 12. Microinjected antibodies against the cytoplasmic tail of p23 decorate the p23 protein in vivo and inhibit the transport of VSV-G through the intermediate compartment. Vero cells were infected with VSV tsO45 and the tsO45-G protein was accumulated in the ER at 39.5°C (*a–e*), in the intermediate compartment at 15°C (*f*) or in the TGN at 20°C (*g*). Cells were microinjected with CT (5 mg/ml IgG-CT), with Fab fragments of these antibodies (2.6 mg/ml Fab-CT), or with nonspecific antibodies (10 mg/ml control IgG). 30 min after injection, the temperature was shifted to 31°C and cells were fixed after 60 min (*a–d*) or after different times (*e–g*). Micrographs *a* and *b,* and *c* and *d* show two identical microinjection experiments, graphs *e–g* show the quantitation of surface (VSV-G) fluorescence as a function of time. Microinjected CT decorated the p23 protein in vivo (*a* and *c*, *arrowheads*). After 60 min at permissive temperature, surface fluorescence was lower in microinjected cells than in neighboring, non-microinjected cells (*b* and *d*). Intracellular tsO45-G partially colocalized with p23 in microinjected cells (*b* and *d*, *arrowheads*), but also accumulated in structures that were negative for p23 (*b* and *d*, *arrows*). Microinjected CT (*e* and *f*, ▲), but not monovalent Fab fragments (*e*, ●), or control antibodies (*e* and *f*, ▲) inhibited the transport of VSV-G from the ER (*e*) or the intermediate compartment (*f*) to the cell surface. Transport of tsO45-G from the TGN to the plasma membrane was not affected by either antibody (*g*). Surface fluorescence was quantitated and each value was normalized to the surface staining obtained for cells injected with control IgG after 90 min (*e* and *f*) or 60 min (*g*). Each value represents the mean of two (*f* and *g*) or three (*e*) independent experiments (>50 cells analyzed in each experiment). The maximal deviation of the mean is indicated. Bar, 15 μm.

Discussion

We have identified, localized, and functionally characterized BHKp23, an integral membrane protein of the emp24/gp25L protein family. Because of their high degree of homology, we consider BHKp23 to be the hamster ortholog of rat/human Tmp21 and rabbit p23 (Blum et al., 1996; Sohn et al., 1996). In yeast cells, emp24p (Schimmöller et al., 1995; Stamnes et al., 1995; Elrod-Erickson and Kaiser, 1996), and erv25p (Belden and Barlowe, 1996) have been previously reported to play a role in protein secretion. In this paper, we show that mammalian p23 is localized to the *cis*-Golgi network/intermediate compartment, and that p23 function is required for biosynthetic membrane transport.

Subcellular Localization of p23

Several lines of evidence demonstrate that p23 localizes to the *cis* side of the Golgi apparatus, in a specific set of membranes that presumably belong to the *cis*-Golgi network/intermediate compartment. Indeed, p23 distributes within typical tubular elements, distal to the ER and proximal to the *cis* side of the Golgi complex (Rambourg and

Clermont, 1990; Schweizer et al., 1990; Lotti et al., 1992). Like ERGIC-53/p58 (Lippincott-Schwartz et al., 1990; Saraste and Svensson, 1991) and other proteins present in the *cis*-Golgi/intermediate compartment (ERD2: Tang et al., 1993; gp74: Alcalde et al., 1994; GM130: Nakamura et al., 1995; p210: Rios et al., 1994; GS28: Subramaniam et al., 1995), p23 does not relocate to the ER after BFA treatment. In addition, p23 colocalizes with newly synthesized VSV-G, but only when VSV-G export from the intermediate compartment is blocked at 15°C (Saraste and Kuismanen, 1984; Schweizer et al., 1990; Lotti et al., 1992). After release of the temperature block, when forward transport resumes, small vesicles containing the G protein are typically devoid of p23.

Although the *cis*-Golgi network/intermediate compartment is relatively ill defined, the generally accepted view is that it serves as a major sorting site where proteins are either retrieved back to the ER or transported forward along the biosynthetic pathway (Warren, 1987; Hauri and Schweizer, 1992; Pelham, 1995). Accordingly, we find a striking colocalization under all conditions tested between p23 and ERD2, the KDEL receptor that moves from the Golgi/intermediate compartment to the ER upon ligand binding (Lewis and Pelham, 1992). In complete agreement with these morphological observations, we find that the bulk ERD2 cofractionates with p23. Since membranes containing p23 appear to be an obligatory step for VSV-G molecules en route to the Golgi, they are likely to represent the first site where the KDEL receptor encounters and binds "escaped" KDEL ligands. The distribution of p23 is different from that of ERGIC-53/p58, since ERGIC-53/p58 localizes to the intermediate compartment and to the ER (Schweizer et al., 1988, 1990; Lippincott-Schwartz et al., 1990; Saraste and Svensson, 1991; H.P. Hauri, personal communication), and because both proteins do not cofractionate. Our observations, thus, suggest that p23 is primarily located on a very distinct set of membranes, which correspond to the *cis*-Golgi network/intermediate compartment, or to a specialized membrane domain within this compartment.

COP I and p23 Membranes

In mammals, rabbit p23 and CHOp24 have been proposed to function as COP and/or cargo receptors, as both proteins are enriched in COP I–coated vesicles generated in vitro (Stamnes et al., 1995; Sohn et al., 1996), and as peptides derived from cytosolic domains of several members of the p24 family are able to recruit COP I coats (Fiedler et al., 1996; Sohn et al., 1996). The proposal that coat receptors exist is attractive because it provides an explanation for the assembly of coats on specific membranes. However, the notion of a receptor remains speculative, since numerous transmembrane cargo proteins also interact via precise sequence motifs with coat components (Trowbridge et al., 1993), including COP I proteins (Cosson and Letourneur, 1994). Indeed, the itinerant protein ERGIC-53/p58, whose cytoplasmic tail has a bona fide dilysine, ER retention signal, has been recently implicated in the membrane association of COP I proteins (Tisdale et al., 1997).

To investigate the possible relationship between COP I and p23, we carried out a complete biochemical and morphological analysis of the distribution of both proteins. Our data show that both β-COP and p23 localize to perinuclear membranes in the Golgi region. However, the distribution of p23 and β-COP does not significantly overlap, except when membrane traffic is arrested at 15°C. After release of this temperature block (when membrane traffic resumes), the degree of colocalization diminishes to steady-state levels. Moreover, we find that vesicular structures appearing immediately after release of this temperature block contain COP I (or VSV-G), as expected, but are typically devoid of p23. These observations strongly suggest that p23 is absent from COP I–coated transport vesicles that carry VSV-G beyond the intermediate compartment. Accordingly, our biochemical and ultrastructural analysis of COP I–coated vesicles generated in vitro, in the presence of GTPγS, demonstrate that p23 is not enriched in purified COP-coated vesicles, and that the cytoplasmic tail of p23 is not required for membrane association of COP I in vitro.

It is difficult at present to provide an explanation for the discrepancy between our findings and those of Stamnes et al. (1995) and Sohn et al. (1996). However, our data strongly suggest that COP I proteins associate to membranes via a p23-independent mechanism, perhaps via other members of the p24 family (Fiedler et al., 1996), or KKXX-CO_2–containing proteins (Cosson and Letourneur, 1994; Tisdale et al., 1997). Indeed, soluble COP I is able to interact with peptides carrying a di-lysine motif in vitro (Cosson and Letourneur, 1994; Fiedler et al., 1996; Sohn et al., 1996), and this property is relevant for protein traffic in vivo (Letourneur et al., 1994). However, it is likely that the interaction of COP I with cytoplasmic tails that carry the di-lysine motif is subject to further regulations in vivo (compare with Letourneur et al., 1995).

Function of p23

Our microinjection data suggest that p23 is involved in forward transport of a transmembrane cargo protein, the ts045 mutant form of the VSV-G glycoprotein. Presumably, p23 is required at the level of the *cis*-Golgi network/intermediate compartment, since forward transport is delayed when the viral protein is preaccumulated at 15°C in the intermediate compartment. The fact that microinjected Fab fragments that decorated the cytoplasmic tail of p23 were not inhibitory, suggests that inhibition is not solely caused by preventing association of soluble factors to the cytoplasmic tail of p23. This is in agreement with the finding that bivalent CT antibodies do not interfere with COP I membrane binding in vitro. The simplest interpretation is that the polyvalent antibody binds to more than one p23 molecule causing their lateral association in the plane of the membrane, and thus interfering with their dynamics. This may directly affect movement of VSV-G through the intermediate compartment, and thus delay its transit, and/or alter the packaging of the viral protein into forming transport vesicles.

Further work will be required to establish the precise function of p23. However, we can speculate that p23 contributes to the structure of the *cis*-Golgi network/intermediate compartment. The p23 protein is a relatively abundant cellular protein that can be visualized by protein stain

on gels of total cellular extracts, and which can be quantitatively recovered after fractionation with a high enrichment (≈50-fold). Since only a small subset of membranes in the fraction contain p23 (≈10–20%), and because these are decorated to a high extent by immunogold particles, p23 must be highly enriched in these membranes. In fact, our morphometric studies indicate that the density of p23 in these membranes is ≈12,500 molecules/μm^2 membrane surface area. For a comparision, the density of spike glycoprotein molecules in the membrane of enveloped viruses was estimated to be ≈22,500 molecules/μm^2, a value in the same range as estimated for integral membrane proteins in intracellular membranes (≈30,000 molecules/μm^2; Quinn et al., 1984). Moreover, caveolin, which is a major structural component of caveolae, was estimated to be present in caveolar membranes at a density of 8,000 molecules/μm^2 (Dupree et al., 1993). We can therefore conclude that p23 is a, if not the, major integral protein of these membranes. These observations, together with the fact that p23 displays heptad repeats of hydrophobic amino acids predicted to form coiled-coil interactions, suggest that p23 contributes to membrane organization and/or dynamics via protein–protein interactions.

So far, p23 is the only member of the p24 family that has been localized in mammalian cells (this work and Sohn et al., 1996). The cellular distribution of other members of the family remains to be established. Clearly, future studies will be required to determine whether members of the p24 family may or may not fulfill similar functions at different subcellular locations or act synergistically at the same transport steps. At present, however, our data strongly suggest that p23-rich membrane domains (presumably involving coiled-coil type interactions) control the dynamics and organization of the *cis*-Golgi network/intermediate compartment, and thereby mediate vesicle formation and trafficking of a transmembrane protein to the Golgi complex.

We thank M.-H. Beuchat for expert technical assistance, I. Fialka for the BHK cDNA library, J. Frey for DNA sequencing, and F. Gu for help with in vitro binding assays. We are grateful to T. Kreis for valuable advice and for critical reading of the manuscript. We also thank T. Nilsson and G. Warren for the HeLa cell line stably expressing a myc-tagged version of NAGT I. We are also grateful to G. van der Goot and F. Perez for critical reading of the manuscript.

This work was supported by grant No. 31-37296.93 from the Swiss National Science Foundation (to J. Gruenberg), grant No. 961235 from the National Health and Medical Research Council of Australia (to R.G. Parton), and grant RG 355/94 from the International Human Frontier Science Program (to J. Gruenberg and R.G. Parton). M. Rojo was a recipient of a long-term fellowship of the Human Capital and Mobility Program of the European Community.

Received for publication 24 April 1997 and in revised form 25 September 1997.

References

Alcalde, J., G. Egea, and I.V. Sandoval. 1994. gp74 a membrane glycoprotein of the *cis*-Golgi network that cycles through the endoplasmic reticulum and intermediate compartment. *J. Cell Biol.* 124:649–665.

Allan, V.J., and T.E. Kreis. 1986. A microtubule-binding protein associated with membranes of the Golgi apparatus. *J. Cell Biol.* 103:2229–2239.

Aniento, F., N. Emans, G. Griffiths, and J. Gruenberg. 1993. Cytoplasmic dynein-dependent vesicular transport from early to late endosomes. *J. Cell Biol.* 123:1373–1387.

Aniento, F., F. Gu, R.G. Parton, and J. Gruenberg. 1996. An endosomal β-COP is involved in the pH-dependent formation of transport vesicles destined for late endosomes. *J. Cell Biol.* 133:29–41.

Ansorge, W., and R. Pepperkok. 1988. Performance of an automated system for capillary microinjection into living cells. *J. Biochem. Biophys. Methods.* 16: 283–292.

Belden, W.J., and C. Barlowe. 1996. Erv25p, a component of COPII-coated vesicles, forms a complex with emp24p that is recquired for efficient endoplasmic reticulum to Golgi transport. *J. Biol. Chem.* 271:26939–26946.

Bergmann, J.E., K.T. Tokuyasu, and S.J. Singer. 1981. Passage of an integral membrane protein, the vesicular stomatitis virus glycoprotein, through the Golgi apparatus en route to the plasma membrane. *Proc. Natl. Acad. Sci. USA.* 78:1746–1750.

Blum, R., P. Feick, M. Puype, J. Vandekerckhove, R. Klengel, W. Nastainczyk, and I. Schulz. 1996. Tmp21 and p24A, two type I proteins enriched in pancreatic microsomal membranes, are members of a protein family involved in vesicular trafficking. *J. Biol. Chem.* 271:17183–17189.

Bomsel, M., R.G. Parton, S.A. Kuznetsov, T.A. Schroer, and J. Gruenberg. 1990. Microtubule- and motor-dependent fusion in vitro between apical and basolateral endocytic vesicles from MDCK cells. *Cell.* 62:719–731.

Celis, J.E., B. Gesser, H.H. Rasmussen, P. Madsen, H. Leffers, K. Dejgaard, B. Honoré, E. Olsen, G. Ratz, J.B. Lauridsen, et al. 1990. Comprehensive 2 D gel protein databases offer a global approach to the analysis of human cells: the transformed amnion cells (AMA) master database and its link to genome DNA sequence data. *Electrophoresis.* 11:989–1071.

Church, G.M., and W. Gilbert. 1984. Genomic sequencing. *Proc. Natl. Acad. Sci. USA.* 81:1991–1995.

Cole, N.B., N. Sciaky, A. Marotta, J. Song, and J. Lippincott-Schwartz. 1996. Golgi dispersal during microtubule disruption: regeneration of Golgi stacks at peripheral endoplasmic reticulum exit sites. *Mol. Biol. Cell.* 7:631–650.

Cosson, P., and F. Letourneur. 1994. Coatomer interaction with di-Lysine endoplasmic reticulum retention motifs. *Science.* 263:1629–1631.

Dupree, P., R.G. Parton, G. Raposo, T.V. Kurzchalia, and K. Simons. 1993. Caveolae and sorting in the trans-Golgi-network of epithelial cells. *EMBO (Eur. Mol. Biol. Organ.) J.* 12:1597–1605.

Elrod-Erickson, M.J., and C.A. Kaiser. 1996. Genes that control the fidelity of endoplasmic reticulum to Golgi transport identified as suppressors of vesicle budding mutations. *Mol. Biol. Cell.* 7:1043–1058.

Emans, N., J.-P. Gorvel, C. Walter, V. Gerke, R. Kellner, G. Griffiths, and J. Gruenberg. 1993. Annexin II is a major component of fusogenic endosomal vesicles. *J. Cell Biol.* 120:1357–1369.

Evan, G.I., G.K. Lewis, G. Ramsay, and J.M. Bishop. 1985. Isolation of monoclonal antibodies specific for human c-myc proto-oncogene product. *Mol. Cell. Biol.* 5:3610–3616.

Fiedler, K., M. Veit, M.A. Stamnes, and J.E. Rothman. 1996. Bimodal interaction of coatomer with the p24 family of putative cargo receptors. *Science.* 273:1396–1399.

Griffiths, G. 1993. Fine Structure Immunocytochemistry. Springer-Verlag, Berlin-Heidelberg. 452 pp.

Griffiths, G., and K. Simons. 1986. The trans golgi network: sorting at the exit of the Golgi complex. *Science.* 234:438–443.

Griffiths, G., A. McDowall, R. Back, and J. Dubochet. 1984. On the preparation of cryosections for immunocytochemistry. *J. Ulstrastruct. Res.* 89:65–78.

Griffiths, G., M. Ericsson, J. Krijnselocker, T. Nilsson, B. Goud, H.D. Soling, B.L. Tang, S.H. Wong, and W.J. Hong. 1994. Localization of the Lys, Asp, Glu, Leu tetrapeptide receptor to the Golgi complex and the intermediate compartment in mammalian cells. *J. Cell Biol.* 127:1557–1574.

Griffiths, G., R. Pepperkok, J.K. Locker, and T.E. Kreis. 1995. Immunocytochemical localization of β-COP to the ER-Golgi boundary and the TGN. *J. Cell Sci.* 108:2839–2856.

Gruenberg, J., and J.-P. Gorvel. 1993. In vitro reconstitution of endocytic vesicle fusion. *In* Protein Targeting: A Practical Approach. A.I. Magee, and T. Wileman, editors. Oxford University Press. Oxford. 187–215.

Gruenberg, J., and K.E. Howell. 1985. Immuno-isolation of vesicles using antigenic sites either located on the cytoplasmic or the exoplasmic domain of an implanted viral protein. A quantitative analysis. *Eur. J. Cell Biol.* 38:312–321.

Gruenberg, J., and F.R. Maxfield. 1995. Membrane transport in the endocytic pathway. *Curr. Opin. Cell Biol.* 7:552–563.

Gruenberg, J., G. Griffiths, and K.E. Howell. 1989. Characterization of the early endosome and putative endocytic carrier vesicles in vivo and with an assay of vesicle function in vitro. *J. Cell Biol.* 108:1301–1316.

Hauri, H.P., and A. Schweizer. 1992. The endoplasmic reticulum-Golgi intermediate compartment. *Curr. Opin. Cell Biol.* 4:600–608.

Jackson, M.R., T. Nilsson, and P.A. Peterson. 1990. Identification of a consensus motif for retention of transmembrane proteins in the endoplasmic reticulum. *EMBO (Eur. Mol. Biol. Organ.) J.* 9:3153–3162.

Klausner, R.D., J.G. Donaldson, and J. Lippincott-Schwartz. 1992. Brefeldin A: Insights into the control of membrane traffic and organelle structure. *J. Cell Biol.* 116:1071–1080.

Kozak, M. 1989. The scanning model for translation: an update. *J. Cell Biol.* 108:229–241.

Kreis, T.E. 1986. Microinjected antibodies against the cytoplasmic domain of vesicular stomatitis virus glycoprotein block its transport to the cell surface. *EMBO (Eur. Mol. Biol. Organ.) J.* 5:931–941.

Kreis, T.E., and H.F. Lodish. 1986. Oligomerization is essential for transport of vesicular stomatitis viral glycoprotein to the cell surface. *Cell.* 46:929–937.

Kreis, T.E., M. Lowe, and R. Pepperkok. 1995. COPs regulating membrane traffic. *Annu. Rev. Cell Dev. Biol.* 11:677–706.

Laemmli, U.K. 1970. Cleavage of structural proteins during the assembly of the head of bacteriophage T4. *Nature.* 227:680–685.

Letourneur, F., E.C. Gaynor, S. Hennecke, C. Demolliere, R. Duden, S.D. Emr, H. Riezman, and P. Cosson. 1994. Coatomer is essential for retrieval of dilysine-tagged proteins to the endoplasmic reticulum. *Cell.* 79:1199–1207.

Letourneur, F., S. Hennecke, C. Demolliere, and P. Cosson. 1995. Steric masking of a dilysine endoplasmic reticulum retention motif during assembly of the human high affinity receptor for immunoglobulin E. *J. Cell Biol.* 129: 971–978.

Lewis, M.J., and H.R.B. Pelham. 1992. Ligand-induced redistribution of a human KDEL receptor from the Golgi complex to the endoplasmic reticulum. *Cell.* 68:353–364.

Lippincott-Schwartz, J., J.G. Donaldson, A. Schweizer, E. Berger, H.P. Hauri, L.C. Yuan, and R.D. Klausner. 1990. Microtubule-dependent retrograde transport of proteins into the ER in the presence of brefelding A reveals an ER recycling pathway. *Cell.* 60:821–836.

Lotti, L.V., M.R. Torrisi, M.C. Pascale, and S. Bonatti. 1992. Immunocytochemical analysis of the transfer of vesicular stomatitis virus G glycoprotein from the intermediate compartment to the Golgi complex. *J. Cell Biol.* 118:43–50.

Lowe, M., and T.E. Kreis. 1996. In vivo assembly of coatomer, the COP-I coat precursor. *J. Biol. Chem.* 271:30725–30730.

Ludwig, T., G. Griffiths, and B. Hoflack. 1991. Distribution of newly synthesized lysosomal enzymes in the endocytic pathway of normal rat kidney cells. *J. Cell Biol.* 115:1561–1572.

Luzio, J.P., B. Brake, G. Banting, K.E. Howell, P. Braghetta, and K.K. Stanley. 1990. Identification, sequencing and expression of an integral membrane protein of the *trans*-Golgi network (TGN38). *Biochem. J.* 270:97–102.

Nakamura, N., C. Rabouille, R. Watson, T. Nilsson, N. Hui, P. Slusarewicz, T.E. Kreis, and G. Warren. 1995. Characterization of a *cis*-Golgi matrix protein, GM130. *J .Cell Biol.* 131:1715–1726.

Nielsen, H., J. Engelbrecht, S. Brunak, and G. von Heijne. 1997. Identification of prokaryotic and eukaryotic signal peptides and prediction of their cleavage sites. *Protein Eng.* 10:1–6.

Nilsson, I.M., and G. von Heijne. 1993. Determination of the distance between the oligosaccharyltransferase active site and the endoplasmic reticulum membrane. *J. Biol. Chem.* 268:5798–5801.

Nilsson, T., M. Pypaert, M.H. Hoe, P. Slusarewicz, E.G. Berger, and G. Warren. 1993. Overlapping distribution of two glycosyltransferases in the Golgi apparatus of HeLa cells. *J. Cell Biol.* 120:5–13.

Oprins, A., R. Duden, T.E. Kreis, H.J. Geuze, and J.W. Slot. 1993. β-COP localizes mainly to the *cis*-Golgi side in exocrine pancreas. *J. Cell Biol.* 121:49–59.

Orci, L., V. Malhotra, M. Amherdt, T. Serafini, and J.E. Rothman. 1989. Dissection of a single round of vesicular transport: sequential intermediates for intercisternal movements in the Golgi stack. *Cell.* 56:357–368.

Orci, L., D.J. Palmer, M. Ravazzola, A. Perrelet, M. Amherdt, and J.E. Rothman. 1993. Budding from Golgi membranes requires the coatomer complex of non-clathrin coat proteins. *Nature.* 362:648–652.

Palade, G.E. 1975. Intracellular aspects of the process of protein synthesis. *Science.* 189:347–358.

Pelham, H.R.B. 1995. Sorting and retrieval between the endoplasmic reticulum and Golgi apparatus. *Curr. Opin. Cell Biol.* 7:530–535.

Pepperkok, R., J. Scheel, H. Horstmann, H.P. Hauri, G. Griffiths, and T.E. Kreis. 1993. β-COP is essential for biosynthetic membrane transport from the endoplasmic reticulum to the Golgi complex in vivo. *Cell.* 74:71–82.

Pevsner, J., and R.H. Scheller. 1994. Mechanisms of vesicle docking and fusion: insights from the nervous system. *Curr. Opin. Cell Biol.* 6:555–560.

Pryer, N.K., L.J. Wuestehube, and R. Schekman. 1992. Vesicle-mediated protein sorting. *Annu. Rev. Biochem.* 61:12336–13361.

Quinn, P., G. Griffiths, and G. Warren. 1984. Density of newly synthesized plasma membrane proteins in intracellular membranes II. Biochemical studies. *J. Cell Biol.* 98:2142–2147.

Rambourg, A., and Y. Clermont. 1990. Three-dimensional electron microscopy: structure of the Golgi apparatus. *Eur. J. Cell Biol.* 51:189–200.

Rios, R.M., A.M. Tassin, C. Celati, C. Antony, M.C. Boissier, J.C. Homberg, and M. Bornens. 1994. A peripheral protein associated with the *cis*-Golgi network redistributes in the intermediate compartment upon brefeldin A treatment. *J. Cell Biol.* 125:997–1013.

Robinson, L.J., F. Aniento, and J. Gruenberg. 1997. NSF is required for transport from early to late endosomes. *J. Cell Sci.* In press.

Rogalski, A.A., and S.J. Singer. 1984. Associations of elements of the Golgi apparatus with microtubules. *J. Cell Biol.* 99:1092–1100.

Rothman, J.E. 1994. Mechanism of intracellular protein transport. *Nature.* 372: 55–63.

Saraste, J., and E. Kuismanen. 1984. Pre- and post-Golgi vacuoles operate in the transport of Semliki Forest virus membrane glycoproteins to the cell surface. *Cell.* 38:535–549.

Saraste, J., and K. Svensson. 1991. Distribution of the intermediate elements operating in ER to Golgi transport. *J. Cell Sci.* 100:415–430.

Scheel, J., R. Pepperkok, M. Lowe, G. Griffiths, and T.E. Kreis. 1997. Dissociation of coatomer from membranes is required for brefeldin A–induced transfer of Golgi enzymes to the endoplasmic reticulum. *J. Cell Biol.* 137:319–333.

Schimmöller, F., B. Singerkruger, S. Schroder, U. Kruger, C. Barlowe, and H. Riezman. 1995. The absence of emp24p, a component of ER-derived COPII-coated vesicles, causes a defect in transport of selected proteins to the Golgi. *EMBO (Eur. Mol. Biol. Organ.) J.* 14:1329–1339.

Schweizer, A., J.A.M. Fransen, T. Bachi, L. Ginsel, and H.P. Hauri. 1988. Identification, by a monoclonal antibody, of a 53-kD protein associated with a tubular-vesicular compartment at the *cis*-side of the Golgi apparatus. *J. Cell Biol.* 107:1643–1653.

Schweizer, A., J.A. Fransen, K. Matter, T.E. Kreis, L. Ginsel, and H.P. Hauri. 1990. Identification of an intermediate compartment involved in protein transport from endoplasmic reticulum to Golgi apparatus. *Eur. J. Cell Biol.* 53:185–196.

Serafini, T., G. Stenbeck, A. Brecht, F. Lottspeich, L. Orci, J.E. Rothman, and F.T. Wieland. 1991. A coat subunit of Golgi-derived non-clathrin coated vesicles with homology to the clathrin-coated vesicle coat protein β-adaptin. *Nature.* 349:215–220.

Sohn, K., L. Orci, M. Ravazzola, M. Amherdt, M. Bremser, F. Lottspeich, K. Fiedler, J.B. Helms, and F.T. Wieland. 1996. A major transmembrane protein of Golgi-derived COPI-coated vesicles involved in coatomer binding. *J. Cell Biol.* 135:1239–1248.

Sönnichsen, B., R. Watson, H. Clausen, T. Misteli, and G. Warren. 1996. Sorting by COP I–coated vesicles under interphase and mitotic conditions. *J .Cell Biol.* 134:1411–1425.

Stamnes, M.A., M.W. Craighead, M.H. Hoe, N. Lampen, S. Geromanos, P. Tempst, and J.E. Rothman. 1995. An integral membrane component of coatomer-coated transport vesicles defines a family of proteins involved in budding. *Proc. Natl. Acad. Sci. USA.* 92:8011–8015.

Subramaniam, V.N., J. Krijnselocker, B.L. Tang, M. Ericsson, A.R.B. Yusoff, G. Griffiths, and W.J. Hong. 1995. Monoclonal antibody HFD9 identifies a novel 28 kDa integral membrane protein on the cis-Golgi. *J. Cell Sci.* 108: 2405–2414.

Tang, B.L., S.H. Wong, X.L. Qi, S.H. Low, and W. Hong. 1993. Molecular cloning, characterization, subcellular localization and dynamics of p23, the mammalian KDEL receptor. *J. Cell Biol.* 120:325–338.

Tang, B.L., S.H. Low, and W.J. Hong. 1995. Differential response of resident proteins and cycling proteins of the Golgi to brefeldin A. *Eur. J. Cell Biol.* 68:199–205.

Tisdale, E.J., H. Plutner, J. Matteson, and W.E. Balch. 1997. p53/58 binds COPI and is required for selective transport through the early secretory pathway. *J. Cell Biol.* 137:581–593.

Trowbridge, I.S., J.F. Collawn, and C.R. Hopkins. 1993. Signal-dependent membrane protein trafficking in the endocytic pathway. *Annu. Rev. Cell Biol.* 9:129–161.

Wada, I., D. Rindress, P.H. Cameron, W.J. Ou, J.J. Doherty, D. Louvard, A.W. Bell, D. Dignard, D.Y. Thomas, and J.J.M. Bergeron. 1991. SSR alpha and associated calnexin are major calcium binding proteins of the endoplasmic reticulum membrane. *J. Biol. Chem.* 266:19599–19610.

Warren, G. 1987. Signals and salvage sequences. *Nature.* 327:17–18.